Chemical Characterization of Organosulfates in Secondary Organic Aerosol Derived from the Photooxidation of Alkanes

M. Riva[1], T. Da Silva Barbosa[2,3], Y.-H. Lin[1,a], E. A. Stone[4], A. Gold[1], and J. D. Surratt[1,*]

[1]Department of Environmental Sciences and Engineering, Gillings School of Global Public Health, The University of North Carolina at Chapel Hill, Chapel Hill, NC, USA

[2] CAPES Foundation, Brazil Ministry of Education, Brasilia, DF 70.040-020, Brazil

[3]Departamento de Química, Instituto de Ciências Exatas, Universidade Federal Rural do Rio de Janeiro, Seropédica, Brazil

[4]Department of Chemistry, University of Iowa, Iowa City, IA 52242, United States

[a] now at: Michigan Society of Fellows, Department of Chemistry, University of Michigan, Ann Arbor, MI, USA

* To whom correspondence should be addressed.

Jason D. Surratt, Department of Environmental Sciences and Engineering, Gillings School of Global Public Health, University of North Carolina at Chapel Hill, Chapel Hill, NC 27599 USA. Tel: 1-(919)-966-0470; Fax: (919)-966-7911; Email: surratt@unc.edu

The authors declare no conflict of interest.

Abstract

We report the formation of aliphatic organosulfates (OSs) in secondary organic aerosol (SOA) from the photooxidation of C_{10} – C_{12} alkanes. The results complement those from our laboratories reporting the formation of OSs and sulfonates from gas-phase oxidation of polycyclic aromatic hydrocarbons (PAHs). Both studies strongly support the formation of OSs from the gas-phase oxidation of anthropogenic precursors, as hypothesized on the basis of recent field studies in which aromatic and aliphatic OSs were detected in fine aerosol collected from several major urban locations. In this study, dodecane, cyclodecane and decalin, considered to be important SOA precursors in urban areas, were photochemically oxidized in an outdoor smog chamber in the presence of either non-acidified or acidified ammonium sulfate seed aerosol. Effects of acidity and relative humidity on OS formation were examined. Aerosols collected from all experiments were characterized by ultra performance liquid chromatography coupled to electrospray ionization high-resolution quadrupole time-of-flight mass spectrometry (UPLC/ESI-HR-QTOFMS). Most of the OSs identified could be explained by formation of gaseous epoxide precursors with subsequent acid-catalyzed reactive uptake onto sulfate aerosol and/or heterogeneous reactions of hydroperoxides. The OSs identified here were also observed and quantified in fine urban aerosol samples collected in Lahore, Pakistan, and Pasadena, CA, USA. Several OSs identified from the photooxidation of decalin and cyclodecane are isobars of known monoterpene organosulfates, and thus care must be taken in the analysis of alkane-derived organosulfates in urban aerosol.

1. Introduction

Atmospheric fine aerosol ($PM_{2.5}$, aerosol with aerodynamic diameter ≤ 2.5 μm) plays a major role in scattering and absorption of solar radiation, which impacts global climate (Kroll and Seinfeld, 2008; Stevens and Boucher, 2012). $PM_{2.5}$ also participates in heterogeneous chemical reactions, affecting the abundance and distribution of atmospheric trace gases (Hallquist et al., 2009). Human exposure to $PM_{2.5}$ is associated with respiratory and cardiovascular diseases (Elder and Oberdorster, 2006).

Typically, the largest mass fraction of $PM_{2.5}$ is organic, dominated by secondary organic aerosol (SOA) formed by the oxidation of volatile organic compounds (VOCs). Although SOA contributes a large fraction (20–90%, depending on location) of total $PM_{2.5}$ mass, current models predict less SOA than is generally observed during field measurements (Kroll and Seinfeld, 2008; Hallquist et al., 2009). The omission of intermediate volatility organic compounds (IVOC) as SOA precursors, such as alkanes or polycyclic aromatic hydrocarbons (PAHs), could contribute in part to the underestimation of SOA mass observed in urban areas (Robinson et al., 2007; Tkacik et al., 2012). Long-chain alkanes are important anthropogenic pollutants emitted by combustion and vehicular sources representing up to 90% of the anthropogenic emissions in certain urban areas (Fraser et al., 1997, Gentner et al., 2012). In the atmosphere, they are rapidly depleted by reaction with OH and NO_3 radicals (Atkinson, 2000) yielding a large variety of oxygenated compounds (Lim and Ziemann, 2005; 2009; Yee et al., 2012; 2013), which could lead to SOA formation (Lim and Ziemman, 2009; Loza et al., 2014). SOA yields have been measured for C_7-C_{25} alkanes having linear, branched and cyclic structures (Lim and Ziemman, 2009; Presto et al., 2010; Tkacik et al., 2012; Loza et al., 2014; Hunter et al., 2014). Structure plays a key role in SOA yield, which increases with carbon number or the presence of cyclic features and tends to decrease with branching as

gas-phase fragmentation predominates (Lambe et al., 2012; Carrasquillo et al., 2014; Loza et al., 2014; Hunter et al., 2014).

The presence of organosulfates (OSs) has been demonstrated in several atmospheric compartments, including atmospheric aerosol (Iinuma et al., 2007; Gómez-González et al., 2008; Hawkins et al., 2010; Hatch et al., 2011; Kristensen et al., 2011; Stone et al., 2012; Shalamzari et al., 2013; Hansen et al., 2014; Liao et al., 2015), rain (Altieri et al., 2009), clouds and fog (Pratt et al., 2013; Boone et al., 2015), and several studies indicate that OSs could contribute to a substantial fraction (up to 30%) of the organic mass measured in ambient $PM_{2.5}$ (Surratt et al., 2008; Tolocka and Turpin, 2012).

Although the variety of OSs identified from field measurements is quite large (Surratt et al., 2008; Tao et al., 2014; Wang et al., 2015; Kuang et al., 2016), only a few OS precursors have been unequivocally identified through laboratory studies. OSs have been generated in SOA in smog chambers from OH, NO_3 or O_3 oxidation of BVOCs, including isoprene (Surratt et al., 2007; Ng et al., 2008), 2-methyl-3-buten-2-ol (MBO) (Zhang et al., 2012; Mael et al., 2015), unsaturated aldehydes (Schindelka et al., 2013; Shalamzari et al., 2014; Shalamzari et al., 2015), monoterpenes (Iinuma et al., 2007; Iinuma et al., 2009; Surratt et al., 2008), and sesquiterpenes (Liggio et al., 2006; Surratt et al., 2008; Iinuma et al., 2009; Noziere et al., 2010; Chan et al., 2011) in the presence of acidified sulfate aerosol. However, the large number of unidentified OSs having C_2 to C_{25} skeletons observed in recent field studies are clearly not derived from BVOC precursors, and suggest alkanes and aromatics as a major source of hitherto unrecognized of OS precursors (Tao et al., 2014; Wang et al., 2015; Kuang et al., 2016). Ma et al. (2014) have recently shown that the contribution of aromatic OSs could represent up to two-thirds of the OSs identified in Shanghai. Aliphatic OSs were identified in the ambient samples from urban locations (Tao et al., 2014; Wang et al., 2015; Kuang et al., 2016), suggesting that gas-phase oxidation of long-chain or cyclic alkanes could be an

97 important source of OSs (Tao et al., 2014). At present, lack of authentic standards prevents
98 quantitation of the OSs contribution to $PM_{2.5}$ mass, underscoring the need to better identify
99 the OS precursors.

100 Studies on the impact of NO_x and O_3 on SOA formation from oxidation of long-chain
101 alkanes (Loza et al., 2014; Zhang et al., 2014) have shown that the presence of NO_x tends to
102 reduce SOA formation by reaction of peroxy radicals (RO_2) with NO, to yield alkoxy radicals
103 (RO). For alkanes containing fewer than 10 carbons, the fragmentation/decomposition of RO
104 radicals will produce higher volatility species (e.g., small carbonyls), which suppresses or
105 reduces SOA formation (Lim and Ziemann, 2005, 2009). Recent studies have shown that
106 increased aerosol acidity is a key variable in enhancing SOA formation through acid-
107 catalyzed reactive uptake and multiphase chemistry of oxidation products derived from
108 biogenic VOCs (BVOCs) such as isoprene (Surratt et al., 2010) and α-pinene (Iinuma et al.,
109 2009). Formation of highly oxidized products, including OSs, demonstrates the importance of
110 heterogeneous processes, such as reactive uptake of epoxides onto acidic sulfate aerosol, in
111 SOA formation (Iinuma et al., 2009; Surratt et al., 2010; Chan et al., 2011; Lin et al., 2014;
112 Shalamzari et al., 2015). OSs may also be formed by either nucleophilic substitution of
113 organic nitrates by sulfate (Darer et al., 2011; Hu et al., 2011) or by heterogeneous oxidation
114 of unsaturated compounds involving sulfate anion radicals (Noziere et al., 2010; Schindelka et
115 al., 2013; Schone et al., 2014).

116 Formation of OSs from the gas-phase oxidation of the C_{10} alkanes, cyclodecane
117 ($C_{10}H_{20}$) and decalin (bicyclo[4.4.0]decane; $C_{10}H_{18}$), and C_{12} alkane, dodecane ($C_{12}H_{26}$), in
118 the presence of sulfate aerosol under varying acidities is reported in this work. These alkanes
119 were selected based on their potential contribution to atmospheric SOA formation (Hunter et
120 al., 2014). Studies have demonstrated that cyclic compounds ($< C_{12}$) are expected to be more
121 efficient SOA precursors than linear or branched alkanes with the same number of carbons

(Lim and Ziemann, 2005; Pye and Pouliot, 2012). Alkanes ≥ C_{10} are considered as effective SOA precursors, especially when placed in the context of their emission rates (Pye and Pouliot, 2012). Effects of RH and aerosol acidity on OS formation were investigated. SOA collected from outdoor smog chamber experiments was chemically characterized by ultra performance liquid chromatography interfaced to high-resolution quadrupole time-of-flight mass spectrometry equipped with electrospray ionization (UPLC/ESI-HR-QTOFMS). In addition, effect of solvent mixture (methanol vs acetonitrile/toluene) on OS quantification was investigated. Finally, $PM_{2.5}$ samples collected from Lahore, Pakistan and Pasadena, CA, USA were analyzed to detect and quantify OSs identified from the smog chamber experiments.

2. Experimental

2.1 Chamber Experiments. Eighteen experiments were performed at the University of North Carolina (UNC) outdoor smog chamber facility located at Pittsboro, NC. Details of this facility have been previously described (Lee et al., 2004; Kamens et al., 2011). Briefly, it is a 274−m^3 dual chamber divided into two sides by a Teflon film curtain. One side referred as "North Chamber" has an actual volume of 136 m^3, and the other side referred as "South Chamber" has an actual volume of 138 m^3. Prior to each experiment, both sides of the chamber were flushed using rural background air using an exhaust blower for at least 12 hours. Clean air was then injected into both sides of the chamber using a clean air generator to reduce concentrations of background aerosol and VOCs. Experiments were performed under two humidity conditions: at low RH (10−20%) and high RH (40−60%). For experiments conducted at low RH (i.e., dry), the clean air generator was used after the preliminary venting using rural air for approximately 48−72 hours. A scanning mobility particle sizer (SMPS, TSI 3080) was used to measure aerosol size distributions, including number and volume concentrations inside both chambers. Before each experiment, the typical aerosol mass

147 concentration (assuming an aerosol density of 1 g cm^{-3}) background was less than ~ 3 μg m^{-3}
148 in humid conditions and less than ~ 0.2 μg m^{-3} for dry experiments. Either non-acidified or
149 acidified ammonium sulfate seed aerosols were introduced into the chambers by atomizing
150 aqueous solutions of 0.06 M $(NH_4)_2SO_4$ or 0.06 M $(NH_4)_2SO_4$ + 0.06 M H_2SO_4, respectively.
151 After 15 min of atomization, ~ 40 μg m^{-3} of seed aerosol was injected into the chambers.
152 After stabilization of aerosol volume concentrations, Teflon blank filters were collected (47
153 mm diameter, 1.0 μm pore size, Tisch Environmental, EPA $PM_{2.5}$ membrane) over 45 min at
154 a sampling rate of ~ 25 L min^{-1} in order to measure baseline aerosol composition prior to
155 injection of the SOA precursors. None of the aliphatic OSs produced from the oxidation of
156 studied alkanes were detected in the chamber background. Dodecane (Sigma-Aldrich, 99%),
157 cyclodecane (TCI, 94%) or decalin (Sigma-Aldrich, 99%, mixture of *cis* + *trans*) were
158 introduced into both sides of the chamber by passing a N_2 flow through a heated manifold
159 containing a known amount of liquid compound. Concentrations of alkanes were measured
160 online in each side every 10 minutes by a gas chromatograph with a flame ionization detector
161 (GC−FID, Model CP-3800, Varian), calibrated before each experiment with a standard
162 mixture of hydrocarbons. Isopropyl nitrite (IPN) (Pfaltz & Bauer, 97%) was used as an OH
163 radical source (Raff and Finlayson-Pitts, 2010) and was injected into both sides when VOC
164 signals were stable as measured by the GC−FID. O_3 and NO_x concentrations were monitored
165 using UV photometric and chemiluminescent analyzers, respectively (O_3: Model 49P,
166 Thermo-Environmental; NO_x: Model 8101B, Bendix). Both instruments were calibrated as
167 described in previous work (Kamens et al., 2011). Dilution rate for each chamber was
168 monitored by sulfur hexafluoride (SF_6) measured using gas chromatography with electron
169 capture detection (GC−ECD). RH, temperature, irradiance and concentration of O_3 and NO_x
170 were recorded every minute. SOA formation from alkane photooxidation was monitored for
171 all experiments. 2−3 hours following IPN injection, which corresponds to the end of SOA

growth as measured by the SMPS, filter sampling was initiated. For each experiment, two filters from each side of the chamber were collected for 45 min − 2 hours (sampling rate ~ 25 L min^{-1}) to characterize particle-phase reaction products. Based on SOA volume concentrations measured by the SMPS, sampling time was adjusted to obtain an SOA mass of about ~ 100 μ g/filter. Experimental conditions are summarized in Table 1.

2.2 Ambient Aerosol Collection. Five filters collected in Lahore (Pakistan) between January 2007 and January 2008 (Stone et al., 2010) and eight filters collected in Pasadena CA, (USA) during the 2010 California Research at the Nexus of Air Quality and Climate Change (CalNex) field study from 15 May − 15 June 2010 (Hayes et al., 2013), were analyzed for the OSs identified in smog chamber experiments. $PM_{2.5}$ was collected on prebaked quartz fiber filters (QFF, Pall Life Sciences, Tissuquartz, 47 mm for Lahore, 20.3 cm × 25.4 cm for Pasadena) using a medium-volume sampling apparatus at Lahore (URG-3000, Chapel Hill, NC, USA) and a high-volume sampler (Tisch Environmental, Cleves, OH, USA) at Pasadena. As stipulated previously at both urban sites, anthropogenic activities (e.g., vehicular exhaust, industrial sources, cooking, etc.) likely dominated the organic aerosol mass fraction of $PM_{2.5}$ (Stone et al., 2010; Hayes et al., 2013). In addition, Gentner et al. (2012) have reported significant emission of long-chain alkanes during the CalNex field study.

2.3 Filter Extraction. The impact of the solvent mixture on OS quantification was also explored in this work. Filters collected from smog chamber experiments were extracted using two different solvent mixtures. One filter was extracted using 22 mL of high-purity methanol (LC-MS CHROMASOLV-grade, Sigma-Aldrich, ≥ 99.9 %) under 45 min (25 min + 20 min) of sonication at room temperature while the second filter was extracted using 22 mL of a 70/30 (v/v) solvent mixture containing acetonitrile/toluene (CHROMASOLV-grade, for HPLC, Sigma-Aldrich, ≥ 99.9 %). Extracts were then blown dry under a gentle nitrogen stream at ambient temperature (Surratt et al., 2008; Zhang et al., 2011; Lin et al., 2012). Dry

197 extracts were then reconstituted with 150 μL of either a 50:50 (v/v) solvent mixture of
198 methanol and water (MilliQ water) or a 50:50 (v/v) solvent mixture of acetonitrile and water.
199 Filters collected from field studies were extracted using methanol as solvent and following the
200 protocol described above; however, prior to drying, extracts were filtered through 0.2-μm
201 PTFE syringe filters (Pall Life Science, Acrodisc) to remove insoluble particles or quartz
202 filter fibers.
203 **2.4 Chemical Analysis.** Characterization of OSs in chamber experiments was performed
204 using ultra performance liquid chromatography interfaced to a high-resolution quadrupole
205 time-of-light mass spectrometer equipped with an electrospray ionization source (UPLC/ESI-
206 HR-Q-TOFMS, 6500 Series, Agilent) operated in the negative ion mode. Exact operating
207 conditions have been previously described (Lin et al., 2012). 5 μL sample aliquots were
208 injected onto a UPLC column (Waters ACQUITY UPLC HSS T3 column). Octyl sulfate
209 ($C_8H_{17}O_4S^-$; Sigma-Aldrich) and 3-pinanol-2-hydrogen sulfate ($C_9H_{13}O_6S^-$) were used as
210 surrogate standards to quantify the identified aliphatic OSs.
211 **2.5 Total Organic Peroxide Analysis.** The total organic peroxides in the SOA were
212 quantified using an iodometric-spectrophotometric method adapted from Docherty et al.
213 (2005). As described in Surratt et al. (2006), the method employed in this work differs in the
214 choice of extraction solvent: we used a 50:50 (v/v) mixture of methanol and ethyl acetate,
215 rather than pure ethyl acetate. Calibrations and measurements were performed at 470 nm
216 using a Hitachi U-3300 dual beam spectrophotometer. Benzoyl peroxide was used as the
217 standard for quantification of organic peroxides formed from alkane oxidations. The molar
218 absorptivity measured from the calibration curve was ~ 825, which is in excellent agreement
219 with previously reported values (Docherty et al., 2005; Surratt et al., 2006).
220
221

3. Results and Discussion

In the subsequent sections, detailed chemical characterization of OSs identified from the gas-phase oxidation of dodecane, decalin and cyclodecane in the presence of ammonium sulfate aerosol is presented. The presence of OSs was revealed by the appearance of characteristic fragment ions at *m/z* 79.95 ($SO_3^{\bullet/-}$), 80.96 (HSO_3^-) and/or 96.96 (HSO_4^-) in tandem mass spectra (MS^2) (Iinuma et al., 2007; Gómez-González et al., 2008; Surratt et al., 2008; Shalamzari et al., 2013; 2014). Tentative structures, retention times and exact mass measurements of OSs detected in this work are reported in Table S1. The low abundance of some OSs precluded acquisition of high-resolution MS^2 data and thus structures have not been proposed for the low-abundance parent ions.

3.1 Characterization of OSs from Dodecane Photooxidation. Seven OSs, including isobaric compounds, were identified in SOA produced from the gas-phase oxidation of dodecane in the presence of sulfate seed aerosol. None have previously been reported in chamber experiments, although they have recently been observed in ambient fine aerosol samples (Tao et al., 2014; Kuang et al., 2016). Concentrations of the products are reported in Table S2. Three isobaric parent ions with *m/z* 279 ($C_{12}H_{23}O_5S^-$, 279.1254), hereafter referred to as OS-279, were identified in SOA generated from dodecane oxidation in the presence of acidified ammonium sulfate aerosol. Kwok and Atkinson (1995) have reported that OH oxidation of long-chain alkanes preferentially occurred at an internal carbon and thus multiple isomers may be proposed. One such isomer, 6-dodecanone-8-sulfate, is drawn in Figure 1 to represent a proposed structure for OS-279. The MS^2 spectra of the products were identical, having product ions diagnostic for a sulfate ester β to an abstractable proton (Surratt et al., 2008; Gómez-González et al., 2008) at *m/*z 199 ($C_{12}H_{23}O_2^-$, loss of neutral SO_3) and 97 (HSO_4^-), precluding assignment of positional isomerism. Figures 1 and S1 present the MS^2 spectrum of OS-279 and proposed fragmentation pathway, respectively. By chemical

ionization mass spectrometry (CIMS) operating in the negative mode, Yee et al. (2012) identified the formation of hydroperoxides from the oxidation of dodecane under low–NO_x conditions, confirming the predicted $RO_2 - HO_2$ reaction pathway in the low–NO_x regime. First-generation hydroperoxides ($C_{12}H_{26}O_2$) can undergo further oxidation by reaction with OH to form either more highly oxidized products, such as dihydroperoxides ($C_{12}H_{26}O_4$), or semi-volatile products ($C_{12}H_{24}O$) (Yee et al., 2012). In addition, hydroperoxides can be photolyzed to alkoxy radicals (RO) undergoing additional transformation to form more highly oxidized products. Low-volatility products could then condense onto sulfate aerosols and undergo further heterogeneous reactions (Schilling Fahnestock et al., 2015) leading to OSs as discussed below. In our study, OH radicals were formed from IPN photolysis without additional injection of NO. Under these conditions, RO_2 chemistry is dominated by RO_2 + HO_2 and/or RO_2 + RO_2 reactions as discussed by Raff and Finlayson-Pitts (2010). Although RO_2 radicals could also react with NO formed by either IPN or NO_2 photolysis, formation of ozone under chamber conditions (0.3-0.6 ppm, depending on the concentration of IPN injected, Table 1) would rapidly quench NO (Atkinson et al., 2000). Therefore, RO_2 + NO reactions are not expected to be significant. In addition, total organic peroxide aerosol concentrations, presented in Table 1, reveal that organic peroxides account (on average) for 28 % of the SOA mass measured in the different experiments in support of a significant contribution of RO_2 + RO_2/HO_2 and/or RO_2 autoxidation to SOA formation from alkane oxidations.

Carbonyl hydroperoxide ($C_{12}H_{24}O_3$), which has been identified in the gas phase by Yee et al. (2012), is likely involved in acid-catalyzed heterogeneous reactions onto sulfate aerosol. Heterogeneous chemistry of gas-phase organic peroxides has been previously suggested to explain the formation of certain OSs and tetrols (Riva et al., 2016). Acid-catalyzed perhydrolysis of hydroperoxides followed by reaction with sulfate anion radicals

could also be possible route to the formation of OS-279 (Figure 1). OS-279 generated from the reactive uptake of the corresponding epoxide ($C_{12}H_{24}O$) has been considered but the composition of OS-279 (1 DBE) is inconsistent with reactive uptake of an epoxide. However, further investigation is required to better understand how acidified sulfate seed aerosol takes up organic peroxides from the gas phase and how particle-phase reactions might degrade organic peroxides into OSs. It should be mentioned that photooxidation of dodecane has also been investigated using an additional injection of NO (200 ppb) prior IPN injection. In this experiment SOA formation was significantly reduced as well as the OS concentrations (factor of 3-4), confirming that NO strongly impacts the formation of OSs, such as OS-279.

3.2 Characterization of OSs from Decalin Photooxidation. Gas-phase oxidation of cyclic alkanes at room temperature and atmospheric pressure has received less attention than linear or branched alkanes. However, recent studies have demonstrated that oxidations of cyclic alkanes by OH radicals produce less−volatile oxygenated compounds and have larger SOA yields (Lim and Ziemann, 2005; Lambe et al., 2012; Tkacik et al., 2012; Yee et al., 2013; Hunter et al., 2014; Loza et al., 2014). Significant formation of OSs (up to 1 μg m^{-3}) and SOA were observed in all experiments of decalin photooxidation (Tables 1 and S3), revealing the high potential for bicyclic alkanes to form OSs. All OSs (25 OSs including isomeric/isobaric structures) identified from the oxidation of decalin in the presence of ammonium sulfate aerosol have been observed in ambient aerosol, underscoring the potential importance of alkanes to OS formation in urban areas (Tao et al., 2014; Wang et al., 2015; Kuang et al., 2016). MS^2 spectra were obtained for all OSs identified from decalin oxidation, except for parent ions at *m/z* 195.0697 (OS-195) and 299.0805 (OS-299). All of the parent ions show an intense product ion at *m/z* 96.96, indicative of an aliphatic sulfate ester. Retention times and tentative structural assignments are given in Table S1.

296 Figures 2 and S2 present MS^2 spectra and fragmentation schemes of selected parent
297 ions at *m/z* 265.0752 (OS-265), 269.0696 (OS-269), 295.0494 (OS-295) and 326.0554 (OS-
298 326). MS^2 spectra and fragmentation schemes of other OSs are reported in Figure S3-S7.
299 These selected OSs exhibit specific fragmentation patterns and were, as described in the next
300 section, quantified and characterized in the fine urban aerosol samples. The different reaction
301 pathways presented below, are separated based on OSs that are generated from branching
302 reactions of a common transient. Four isomers of OS-265 with composition $C_{10}H_{17}O_6S^-$ were
303 identified in decalin-derived SOA collected from all experiments. With regard to components
304 of ambient SOA, it is important to mention that the formation of isobaric OSs with the same
305 elemental composition of $C_{10}H_{17}O_6S^-$ isobars have also been previously identified in SOA
306 produced from the gas-phase oxidation of monoterpenes (Liggio et al., 2006; Surratt et al.,
307 2008) and are not unique to decalin oxidation. The product ion at nominal *m/z* 97 (HSO_4^-)
308 and loss of neutral SO_3 in the MS^2 spectrum (Figure 2a) is consistent with an aliphatic OS
309 having a labile proton in a β position (Attygalle et al., 2001). Absence of product ions
310 corresponding to a loss of a terminal carbonyl ($-CO$) or a carboxyl group ($-CO_2$),
311 respectively (Romero and Oehme, 2005; Shalamzari et al., 2014), and a composition
312 corresponding to 2 double bond equivalencies (DBEs) has thus been attributed to an internal
313 carbonyl group and a six-membered ring. A scheme leading to the structure proposed in
314 Figure 2a is based on the cleavage of the C_1-C_2 decalin bond, followed by reaction with a
315 second O_2 molecule and HO_2 leads to a terminal carbonyl hydroperoxide ($C_{10}H_{18}O_3$) (Yee et
316 al., 2013). $C_{10}H_{18}O_3$ could then further react with OH radicals and lead to an epoxide and
317 sulfate ester by reactive uptake/heterogeneous chemistry (Paulot et al., 2009). OS-265
318 ($C_{10}H_{17}O_6S^-$) could also arise from the acid-catalyzed perhydrolysis of the hydroperoxide
319 ($C_{10}H_{18}O_4$) generated from the reaction of $C_{10}H_{17}O_4^{\bullet}$ + HO_2 (Figure S8, pathway b). The MS^2
320 spectrum for the single parent ion at *m/z* 281 corresponding to the composition $C_{10}H_{17}O_7S^-$

(OS-281) gave product ions expected for a sulfate ester β to a labile proton with 2 DBE, but no additional structural information (Figure S4). The pathway proposed in Figure S8 pathway **b** is based on gas-phase oxidation of a 4-(cyclohexan-2-one)but-1-yl radical followed by reaction with O_2 and a 1,5-H shift (Crounse et al., 2011; Orlando and Tyndall, 2012) and lead to a C_{10}-carbonyl-hydroxyhydroperoxide ($C_{10}H_{18}O_4$). $C_{10}H_{18}O_4$ could then further react with OH radical and by elimination of OH lead to an epoxide (Figure S8, pathway **b**). In addition, OS-281 could arise from acid-catalyzed perhydrolysis of C_{10}-carbonyl dihydroperoxides ($C_{10}H_{18}O_5$) as proposed in Figure S8, pathway **c**. The direction of ring opening of the internal epoxide by reactive uptake to give the final product is arbitrary. Three isobaric parent ions at *m/z* 297 corresponding to the composition $C_{10}H_{17}O_8S^-$ with 2 DBEs were identified. Loss of water, HSO_4^- and SO_3 as a neutral fragment in the MS^2 spectrum of the major isobar (OS-297) is consistent with a hydroxyl-substituted sulfate ester β to a labile proton (Figure S6). The scheme proposed in Figure S8 pathway **c** is based on the oxidation to a 4-(cyclohexan-2-one)but-1-yl radical as in pathway **b**. However, in contrast to pathway **b**, RO_2 formed by the addition of O_2 undergoes a 1,6-H shift (Crounse et al., 2011; Orlando and Tyndall, 2012) followed by addition of a second O_2 molecule, a 1,5-H shift and elimination of OH to yield an epoxide, which leads to a sulfate ester by reactive uptake onto acidified aerosols. The direction of ring opening of the internal alkyl epoxide is arbitrary.

The composition of the parent ion at *m/z* 269.0696 ($C_9H_{17}O_7S^-$) corresponds to one DBE. MS^2 spectrum yields products consistent with a sulfate ester β to an abstractable proton and similar to OS-265, neither a terminal carbonyl nor a carboxyl functional group was detected in the OS-269. As a result, the presence of hydroperoxide and/or hydroxyl substituents is expected in order to satisfy the molecular formulas obtained by the accurate mass measurement. Although ESI-MS in the negative ion mode is not sensitive to multifunctional hydroperoxides and alcohols (Cech and Enke, 2001; Witkowski and Gierczak,

346 2012), this technique is highly sensitive to hydroperoxides and alcohols, which also contain
347 OS groups and give $[M - H]^-$ ions (Surratt et al., 2008; Kristensen et al., 2011; Kundu et al.,
348 2013; Hansen et al., 2014).

349 In Figure 3, tentative pathways leading to the formation of OS-267, OS-269 and OS-
350 285 are proposed. Following analogous mechanisms for low-NO_x conditions (Atkinson, 2000;
351 Yee et al., 2013), abstraction of a proton α to the ring scission of decalin followed by reaction
352 with O_2 leads to the 1-hydroperoxy radical, which in turn can react with another RO_2 radical
353 to yield the corresponding alkoxyl radical ($C_{10}H_{17}O$). Cleavage of the C_1−C_2 decalin bond,
354 followed by reaction with a second O_2 molecule and HO_2 leads to a terminal carbonyl
355 hydroperoxide ($C_{10}H_{18}O_3$). The aldehydic intermediate in the sequence following C_1-C_2 ring
356 scission may be oxidized to the corresponding acyl radical either by photolysis (Wang et al.,
357 2006) or by H-abstraction (Kwok and Atkinson 1995) followed by addition of O_2, reaction
358 with RO_2 or HO_2 and decarboxylation of the resulting acyl-oxy radical (R(O)O) (Chacon-
359 Madrid et al., 2013) to a hydroperoxyperoxy radical ($C_9H_{17}O_4^{\bullet}$). $C_9H_{17}O_4^{\bullet}$ can react via
360 pathway **a** (Figure 3) through a 1,6-H shift (Crounse et al., 2011; Orlando and Tyndall, 2012)
361 followed by elimination of OH resulting in a formation of an epoxide analogous to the
362 formation of isoprene epoxydiol (IEPOX) (Paulot et al., 2009; Mael et al., 2015). The epoxide
363 can then undergo acid-catalyzed ring opening to give OS-269 ($C_9H_{17}O_7S^-$). The MS^2
364 spectrum of OS-285 ($C_9H_{17}O_8S^-$; Figure S5) shows product ions corresponding to HSO_3^-,
365 HSO_4^- and loss of neutral SO_3, in accord with a sulfate ester β to a labile proton, but yields no
366 further structural information. The structure proposed for OS-285 is based on the formation of
367 reaction of the hydroperoxyperoxyl radical intermediate in pathway **b** with RO_2 followed by a
368 1,4-H shift (Rissanen et al., 2015) and addition of O_2 to give a hydroxyhydroperoxyperoxyl
369 radical ($C_9H_{17}O_5^{\bullet}$). $C_9H_{17}O_5^{\bullet}$ could then lead to an epoxide by isomerization (Iinuma et al.,
370 2009; Surratt et al., 2010; Jacobs et al., 2013; Mael et al., 2015) and form OS-285. $C_9H_{17}O_5^{\bullet}$

371 could also react with HO_2 and form the corresponding C_9-hydroxydihydroperoxide
372 ($C_9H_{18}O_5$), which could then undergo heterogeneous reaction and lead to OS-269 (Figure 3,
373 pathway **b**). Finally, a C_9-carbonyl hydroperoxide ($C_9H_{16}O_3$) could also be formed from the
374 RO + O_2 reaction (Figure 3, pathway **c**), which could then further react with OH radicals and
375 lead to a C_9-carbonyl dihydroperoxide ($C_9H_{16}O_5$). Hence, $C_9H_{16}O_5$ could form OS-267
376 ($C_9H_{15}O_7S^-$) from heterogeneous reaction on acidic aerosols.

377 In Figure 4, pathways from an initial 1-peroxy transient are proposed to products
378 designated OS-295, OS-311 and OS-326. Three isobaric ions corresponding to OS-295
379 ($C_{10}H_{15}O_8S^-$) were identified in decalin-derived SOA under all experimental conditions.
380 Figure 2c shows the MS^2 spectrum of the parent ion at *m/z* 295. A product ion at *m/z* 251
381 corresponding to loss of CO_2 (Romero and Oehme, 2005; Shalamzari et al., 2014) is present
382 in addition to product ions consistent with a sulfate ester β to a labile H (Riva et al., 2015).
383 Pathway **a** leads to the structure consistent with the MS^2 spectrum and 3 DBEs required by
384 the composition of the parent ion. The salient features of pathway **a** include oxidation of the
385 RO_2 to 2-decalinone, formation of a C_{10} alkoxy radical followed by ring cleavage of the
386 C_9–C_{10} decalin bond and further RO_2 isomerization (1,8-H shift) leading to a 4-(carboxy
387 cyclohexyl)-1-hydroperoxybut-2-yl radical via RO_2 chemistry. Although considered as a
388 minor reaction pathway (Crounse et al., 2013), the acyloxy radical could lead to the epoxide
389 from the isomerization of the O_2 adduct (Paulot et al., 2009; Yao et al., 2014; Zhang et al.,
390 2015). Further acid-catalyzed ring opening of the epoxide leads to OS-295 ($C_{10}H_{15}O_8S^-$).

391 Two isobaric parent ions with identical MS^2 spectra were observed at *m/z* 311
392 ($C_{10}H_{15}O_9S^-$; Figure S7). The only observed product ion at *m/z* 97 is consistent with a sulfate
393 ester, but not informative with regard to a more refined assignment of molecular structure.
394 Pathway **b** to a hydroperoxide for the parent ion with 3 DBEs is proposed by analogy to the
395 putative hydroperoxide structures of OS-267, OS-269 and OS-285. Pathway **b** is

characterized by a H-abstraction from a carbon at the ring fusion of 2-decalinone leading to formation of an 2-decalinone-6-oxy radical followed by a sequence of ring cleavage, O_2 additions and H-shifts to form a 4-(2,6-cyclohexyl)-2-hydroperoxybutan-1-oxide that can form the sulfate ester on reactive uptake. Abstraction of H1 rather than H6 would lead to an isobaric structure.

Four isobaric ions corresponding to $C_{10}H_{16}NO_9S^-$ with analogous MS^2 spectra (Figure 2d) were detected at nominal mass *m/z* 326. The loss of 63 mass units as neutral HNO_3 (Figure S2d) is in accord with a nitrate ester (Surratt et al., 2008), supported by the absence of product ions from loss of NO or NO_2 (Kitanovski et al., 2012). Although RO_2 + NO reactions are expected to be minor under the conditions used in this work (i.e. NO < 1 ppb, formation of RO radicals or organonitrates cannot be ruled out. Indeed, Ehn et al. (2014) have demonstrated that NO reactions could be competitive at ppb levels. Under our experimental conditions RO_2 + NO, RO_2 + HO_2/RO_2 and RO_2 autoxidation are possible. Therefore, the parent ion at *m/z* 326 could arise from the reaction of the decalin-2-peroxy radical with NO to form decalin-2-nitrate ($C_{10}H_{17}NO_3$) with subsequent reactions shown in Figure 4, pathway **c**. From this point, a sequence of reactions identical to pathway **b** yields the parent OS-326. It is important to mention that the formation of isobaric OSs with the same elemental composition of $C_{10}H_{16}NO_9S^-$ isobars have also been identified in SOA produced from the gas-phase oxidation of monoterpenes (Surratt et al., 2008).

3.3 Characterization of OSs from Cyclodecane Photooxidation. The concentrations of OSs identified from gas-phase oxidation of cyclodecane are reported in Table S4. High levels of OSs were observed in experiments performed under dry conditions with acidified ammonium sulfate seed aerosol. The impact of acidity on OS formation will be discussed in more detail in the following section. The MS^2 spectra of all cyclodecane products show only a single product ion at nominal *m/z* 97 corresponding to bisulfate (Figures S9 – S13), indicating

421 that the oxidation products are sulfate esters β to a labile proton. None of the fragment ions
422 observed in the MS^2 spectrum suggests the presence of a terminal carbonyl or a carboxyl
423 functional group in the cyclodecane-OSs, which is consistent with conservation of the
424 cyclodecane ring. Tentative structures proposed in Table S1 are based on DBE calculations
425 and retention of the cyclodecane ring supported by MS^2 data. Pathways proposed in Figure
426 S14 are initiated by H-abstraction and based on reaction sequences for which precedent has
427 been established: addition of O_2 to cycloalkyl radicals to give RO_2 which either reacts with
428 RO_2 to yield alkoxy radicals (Atkinson and Arey, 2003; Ziemann and Atkinson, 2012) or
429 undergoes intramolecular H-shifts leading to generation of hydroperoxides (Ehn et al., 2014;
430 Jokinen et al., 2014; Mentel et al., 2015). The formation of compounds such as cyclodecanone
431 ($C_{10}H_{18}O$), cyclodecane hydroperoxide ($C_{10}H_{20}O_2$) or cyclodecane hydroxyhydroperoxide
432 ($C_{10}H_{20}O_3$) are proposed as intermediate products leading to epoxy-compounds after
433 additional oxidation/isomerization processes, as presented in Figure S14. In addition
434 $C_{10}H_{20}O_3$, cyclodecane hydroperoxide ketone ($C_{10}H_{18}O_3$) and cyclodecane
435 hydroxyoxohydroperoxide ($C_{10}H_{18}O_4$), proposed as intermediate products, could condense
436 onto wet acidic aerosols and lead to the corresponding OSs through acid-catalyzed
437 perhydrolysis reactions (Figure S14). Since authentic standards are unavailable and the MS^2
438 data do not allow specific structural features to be assigned, the end products in pathways in
439 Figure S14 are arbitrary. Isobars may be explained by *cis*/*trans* epoxide ring opening or the
440 span of an H-shift (1,5-,/1,8-H shifts are possible) (Orlando and Tyndall, 2012). In the case of
441 OS-249, where *cis*/*trans* isomers are not possible; the two isobaric structures may result from
442 different H-shifts. OS-265 and OS-281 are reported here for the first time in chamber studies.
443 **3.4 Impact of Relative Humidity and Acidity on OS Formation.** Experiments were
444 performed under conditions reported in Table 1. As shown in Figure 5 and Tables S2-S4, the
445 presence of acidic aerosols significantly increases OS formation in most cases, as previously

observed for OSs in SOA generated from biogenic sources (Iinuma et al., 2007; Surratt et al., 2007; Chan et al., 2011). Since differences in meteorology could impact experimental results from the outdoor chamber, caution must be exercised in comparing experiments performed on different days. However, same-day, side-by-side experiments allow for clear resolution of the effects of aerosol acidity and seed composition on OS formation. When comparing experiments performed under dry versus wet conditions with acidified ammonium sulfate aerosol, higher RH conditions significantly reduce OS formation, likely attributable to an increase in pH because of dilution by additional particle water. It is important to point out that the effect of varying the aerosol acidity was not cleanly separated from the potential impact of larger concentrations of aerosol sulfate. However, Chan et al. (2011) have demonstrated that the formation of OSs from the oxidation of β-caryophyllene is directly correlated with aerosol acidity ($[H^+]$). Indeed, the authors have changed the acidity of the seed aerosols by adjusting the ratio of the aqueous $(NH_4)_2SO_4/H_2SO_4$ solutions to produce a constant aerosol sulfate concentration of 30 μg m^{-3} across the range acidities.

To better investigate the effect of acidity on OS formation, products were divided in two groups (Figure 5), those whose concentrations were increased by a factor ≥ 2 (Group-1) and ≤ 2 (Group-2). Figure 5 and Tables S2-S4 show that OSs identified from dodecane photooxidation belong to Group-2, with the exception of OS-279. OSs from decalin photooxidation, including OS-195, OS-269 and OS-297 belong to Group-2 as well. OSs can be formed via different pathways, including acid-catalyzed ring-opening reactions of epoxy-containing SOA constituents, reactive uptake of unsaturated compounds into the particle phase, or by reaction with the sulfate anion radical (Rudzinski et al., 2009; Nozière et al., 2010; Schindelka et al., 2013; Schöne et al., 2014). OSs may also result from nucleophilic substitution of nitrate by sulfate (Darer et al., 2011; Hu et al., 2011). The impact of acidity on OS formation arising from the different pathways has been investigated principally for

reactive uptake of epoxy-compounds (Jacobs et al., 2013; Lin et al., 2012; Gaston et al., 2014; Riedel et al., 2015) for which OS formation is strongly enhanced under acidic conditions (Lin et al. (2012). However, a similar enhancement was not observed in our study on PAH-OSs, which were not expected to result from epoxide chemistry (Riva et al., 2015). Based on these observations, the formation of Group-1 OSs are hypothesized to be products of reactive uptake of gas-phase epoxides.

3.5 Impact of Solvent Mixture on OS Quantification. Additional filters were collected from each side of the outdoor chamber and for each experiment to investigate the impact of solvent mixture on OS quantification. Tao et al. (2014) have recently reported that less polar solvents such as an acetonitrile (ACN)/toluene mixture are a better choice for extraction of long alkyl-chain OSs from filters using a nanospray-desorption electrospray ionization mass spectrometry where the extraction occurs *in situ* and the analyses are qualitative. Figure 6 demonstrates that, overall, concentrations of OSs (ng m^{-3}) from the photooxidation of dodecane, decalin and cyclodecane seem to be more efficiently extracted by the ACN/toluene mixture. It is important to note that the concentrations of the aliphatic OSs could be underestimated due to their potential partial re-dissolution in the reconstitution solutions. Tables S2-S4, showing the ratios of the concentrations individual OSs extracted by the ACN/toluene mixture divided by the concentration of OSs extracted by methanol, indicates that all $C_{10}-$ and $C_{12}-$ OS products, including highly oxidized OS, appear more efficiently extracted by the ACN/toluene mixture. For OSs smaller than C_{10}, extraction efficiencies are about the same. As noted above, isobars of OSs identified from the oxidation of alkanes have been observed in SOA generated from the oxidation of monoterpenes that are currently used as tracers for monoterpene SOA chemistry (Hansen et al., 2014; Ma et al., 2014). Hence, in addition to the caution that quantitation of alkane and monoterpene OSs is uncertain in the absence of authentic standards, some monoterpene OSs may be underestimated if not fully

extracted because most studies use methanol as an extraction solvent (Surratt et al., 2008; Iinuma et al., 2009). However, more work is needed to better characterize and elucidate the impact of solvent mixture on the quantitation of biogenic- and anthropogenic-derived OSs, especially compounds > C_{10}, by using internal standards.

3.6 OSs Derived from Alkanes in Ambient Fine Urban Aerosol. Archived fine urban aerosol samples collected at Lahore, Pakistan, and Pasadena, CA, USA were used to evaluate and quantify OSs identified in SOA produced from the photooxidation of alkanes. Filters were initially extracted using methanol and comparison to OSs quantified using another solvent mixture was not possible. As previously mentioned, seven parent ions have been observed in laboratory studies. Therefore, extracted ion chromatograms (EICs) obtained from smog chamber experiments were compared to those obtained from both urban locations to confirm that observed OSs correspond to OSs identified in our lab study. Figures 7 and S15 present the EICs of OSs observed in both ambient and our smog chamber-generated SOA. Table 2 identifies 12 OSs, along with concentrations, present in $PM_{2.5}$ collected from Lahore, Pakistan and Pasadena, CA, USA and also observed in our smog-chamber-generated SOA.

The high concentrations, especially at Lahore (Pakistan) of the OSs measured in the ambient aerosol samples support their use as tracers for SOA produced from the oxidation of alkanes in urban areas. This is consistent with recent proposals (Tao et al., 2014). OS-195 ($C_7H_{15}O_4S^-$), OS-249 ($C_{10}H_{17}O_5S^-$), OS-255 ($C_9H_{19}O_6S^-$), OS-267 ($C_{10}H_{19}O_6S^-$), OS-281 ($C_{10}H_{17}O_7S^-$), OS-299 ($C_{10}H_{19}O_8S^-$), OS-307 ($C_{12}H_{19}O_7S^-$) and OS-311 ($C_{10}H_{15}O_9S^-$) have been recently identified in ambient aerosol collected from the major urban locations Shanghai and Hong Kong (Tao et al., 2014; Wang et al., 2015; Kuang et al., 2016). In the absence of retention times and chromatographic conditions, OS isobars such as OS-249 or OS-279, which are currently assigned to biogenic-derived OSs (Ma et al., 2014), could also arise from anthropogenic sources such as photooxidation of cyclodecane, especially in urban areas.

4. Conclusions

The present study demonstrates the formation of OSs from the photooxidation of alkanes and complements the smog chamber study on formation of OSs and sulfonates from photooxidation of PAHs (Riva et al., 2015). Together, the results strongly support the importance of the contribution of anthropogenic precursors to OS in ambient urban $PM_{2.5}$ proposed on the basis of aromatic and aliphatic OSs in fine aerosol collected from several major urban locations (Kundu et al., 2013, Tao et al., 2014). Chemical characterization of OSs that were identified in SOA arising from the photooxidation of alkanes were performed and tentative structures have been proposed for OSs identified from the photooxidation of decalin, cyclodecane, and dodecane based on composition from exact mass measurement, DBE calculations and the transformations expected from hydroxyl radical oxidation dominated by RO_2/HO_2 chemistry. Enhancement of OS yields in the presence of acidified ammonium sulfate seed is consistent with reactive uptake of gas-phase epoxides as the pathway for OS formation. As previously proposed for IEPOX formation (Paulot et al. 2009), isomerization of RO_2 species to β hydroperoxy alkyl radicals followed by elimination of OH, is a plausible pathway to gas-phase epoxides. It is interesting to note that OS formation through reactive uptake of epoxides have been only observed for cyclic alkanes, which is consistent with the larger concentration of OSs identified from the oxidation of cyclodecane and decalin. However, more work is required to validate pathway(s) leading to the formation of gaseous epoxy-products, since OS formation from other chemical pathways such as nuclophilic substitution of the $–ONO_2$ group by a $–OSO_3$ group cannot be ruled out (Darer et al., 2011; Hu et al., 2011). Of critical importance would be investigations starting from authentic primary or secondary oxidation products suggested in this study as putative intermediates to validate the proposed mechanisms. A novel pathway involving heterogeneous reactions of hydroperoxides followed by hydrolysis/sulfation reactions is proposed to explain the

546 formation of 8 OSs identified in this study; however, more work is also required to examine
547 how acidified sulfate seed aerosols take up organic peroxides from the gas phase and how
548 particle-phase reactions might degrade organic peroxides into low-volatility products such as
549 the OSs.
550

Acknowledgments

The authors thank the Camille and Henry Dreyfus Postdoctoral Fellowship Program in Environmental Chemistry for their financial support. The authors wish also to thank CAPES Foundation, Ministry of Education of Brazil (award no. 99999.000542/2015-06) for their financial support. This study was supported in part by the National Oceanic and Atmospheric Administration (NOAA) Climate Program Office's AC4 program, award no. NA13OAR4310064. The authors wish to thank Kasper Kristensen and Marianne Glasius (Department of Chemistry, Aarhus University, Denmark) who synthesized the 3-pinanol-2-hydrogen sulfate. The authors also thank Tauseef Quraishi, Abid Mahmood, and James Shauer for providing filters collected in Lahore, in addition to the Government of Pakistan, the Pakistani Higher Education Commission, and the United States Agency for International Development (US-AID) for funding field sample collection in Pakistan.

References

Atkinson, R.: Atmospheric chemistry of VOCs and NOx, Atmos. Environ., 34, 2063-2101, 2000.

Atkinson, R., and Arey, J.: Atmospheric degradation of volatile organic compounds, Chem. Rev., 103, 4605-4638, 2003.

Altieri, K.E., Turpin, B.J., and Seitzinger, S.P.: Oligomers, organosulfates, and nitrooxy organosulfates in rainwater identified by ultra-high resolution electrospray ionization FT-ICR mass spectrometry, Atmos. Chem. Phys., 9, 2533-2542, 2009.

Attygalle, A.B., Garcia-Rubio, S., Ta, J., and Meinwald, J.: Collisionally-induced dissociation mass spectra of organic sulfate anions, J. Chem. Soc., Perkin Trans. 2, 4, 498-506, 2001.

Boone, E.J., Laskin, A., Laskin, J., Wirth, C., Shepson, P.B., Stirm, B.H., and Pratt, K.A.: Aqueous processing of atmospheric organic particles in cloud water collected via aircraft sampling, Environ. Sci. Technol., 49, 8523-8530, 2015.

Carrasquillo, A.J., Hunter, J.F., Daumit, K.E., and Kroll, J.H.: Secondary organic aerosol formation via the isolation of individual reactive intermediates: role of alkoxy radical structure, J. Phys. Chem. A, 118, 8807-8816, 2014.

Cech, N.B., and Enke, C.G.: Practical implications of some recent studies in electrospray ionization fundamentals, Mass Spect. Rev., 20, 362-387, 2001.

Chacon-Madrid, H.J., Henry, K.M., and Donahue, N.M.: Photo-oxidation of pinonaldehyde at low NOx: from chemistry to organic aerosol formation, Atmos. Chem. Phys., 13, 3227-3236, 2013.

Chan, M.N., Surratt, J.D., Chan, A.W.H., Schilling, K., Offenberg, J.H., Lewandowski, M., Edney, E.O., Kleindienst, T.E., Jaoui, M., Edgerton, E.S., Tanner, R.L., Shaw, S.L., Zheng, M., Knipping, E.M., and Seinfeld, J.H.: Influence of aerosol acidity on the chemical composition of secondary organic aerosol from β-caryophyllene, Atmos. Chem. Phys., 11, 1735-1751, 2011.

Claeys, M., Wang, W., Ion, A.C., Kourtchev, I., Gelencsér, A., and Maenhaut, W.: Formation of secondary organic aerosols from isoprene and its gas-phase oxidation products through reaction with hydrogen peroxide, Atmos. Environ., 38, 4093-4098, 2004.

601 Crounse, J.D., Paulot, F., Kjaergaard, H.G., and Wennberg, P.O.: Peroxy radical isomerization in the
602 oxidation of isoprene, Phys. Chem. Chem. Phys., 13, 13607–13613, 2011.
603
604 Crounse, J.D., Nielsen, L.B., Jorgensen, S., Kjaergaard, H.G., and Wennberg, P.O.: Autoxidation of
605 organic compounds in the atmosphere, J. Phys. Chem. Lett, 4, 3513-3520, 2013.
606
607 Darer, A.I., Cole-Filipiak, N.C., O'Connor, A.E., and Elrod, M.J.: Formation and stability of
608 atmospherically relevant isoprene-derived organosulfates and organonitrates, Environ. Sci. Technol.,
609 45, 1895–1902, 2011.
610
611 Docherty, K.S., Wu, W., Lim, Y.B., and Ziemann, P.J.: Contributions of organic peroxides to
612 secondary aerosol formed from reactions of monoterpenes with O_3, Environ. Sci. Technol., 39, 4049-
613 4059, 2005.
614
615 Ehn, M., Thornton, J.A., Kleist, E., Sipilä, M., Junninen, H., Pullinen, I., Springer, M., Rubach, F.,
616 Tillmann, R., Lee, B., Lopez- Hilfiker, F., Andres, S., Acir, I.-H., Rissanen, M., Jokinen, T.,
617 Schobesberger, S., Kangasluoma, J., Kontkanen, J., Nieminen, T., Kurten, T., Nielsen, L.B.,
618 Jorgensen, S., Kjaergaard, H.G., Canagaratna, M., Maso, M.D., Berndt, T., Petaja, T., Wahner, A.,
619 Kerminen, V.-M., Kulmala, M., Worsnop, D.R., Wildt, J., and Mentel, T.F.: A large source of low-
620 volatility secondary organic aerosol, Nature, 506, 476–479, 2014.
621
622 Elder, A., and Oberdörster, G.: Translocation and effects of ultrafine particles outside of the lung,
623 Clin. Occup. Environ. Med., 5, 785-796, 2006.
624
625 Fraser, M.P., Cass, G.R., Simoneit, B.R.T, and Rasmussen, R.A.: Air quality model evaluation data
626 for organics. 4. C2-C36 non- aromatic hydrocarbons, Environ. Sci. Technol., 31, 2356-2367, 1997.
627
628 Gaston, C.J., Riedel, T.P., Zhang, Z., Gold, A., Surratt, J.D., and Thornton, J.A: Reactive uptake of an
629 isoprene-derived epoxydiol to submicron aerosol particles, Environ. Sci. Technol., 48, 11178-11186,
630 2014.
631
632 Gentner, D.R., Isaacman, G., Worton, D.R., Chan, A.W.H., Dallmann, T.R., Davis, L., Liu, S., Day,
633 D.A., Russell, L.M., Wilson, K.R., Weber, R., Guha, A., Harley, R.A., and Goldstein, A.H.:
634 Elucidating secondary organic aerosol from diesel and gasoline vehicles through detailed
635 characterization of organic carbon emissions. Proc. Natl. Acad. Sci., 109, 18318−18323, 2012.
636

637 Gómez-González, Y., Surratt, J.D., Cuyckens, F., Szmigielski, R., Vermeylen, R., Jaoui, M.,
638 Lewandowski, M., Offenberg, J.H., Kleindienst, T.E., Edney, E.O., Blockhuys, F., Van Alsenoy, C.,
639 Maenhaut, W., and Claeys, M.: Characterization of organosulfates from the photooxidation of
640 isoprene and unsaturated fatty acids in ambient aerosol using liquid chromatography/(-) electrospray
641 ionization mass spectrometry, J. Mass Spect., 43, 371-382, 2008.
642
643 Hallquist, M., Wenger, J.C., Baltensperger, U., Rudich, Y., Simpson, D., Claeys, M., Dommen, J.,
644 Donahue, N.M., George, C., Goldstein, A.H., Hamilton, J.F., Herrmann, H., Hoffmann, T., Iinuma, Y.,
645 Jang, M., Jenkin, M.E., Jimenez, J.L., Kiendler-Scharr, A., Maenhaut, W., McFiggans, G., Mentel,
646 T.F., Monod, A., Prévôt, A.S.H., Seinfeld, J.H., Surratt, J.D., Szmigielski, R., and Wildt, J.: The
647 formation, properties and impact of secondary organic aerosol: current and emerging issues, Atmos.
648 Chem. Phys., 9, 5155-5236, 2009.
649
650 Hansen, A.M.K., Kristensen, K., Nguyen, Q.T., Zare, A., Cozzi, F., Nøjgaard, J.K., Skov, H., Brandt,
651 J., Christensen, J.H., Ström, J., Tunved, P., Krejci, R., and Glasius, M.: Organosulfates and organic
652 acids in Arctic aerosols: Speciation, annual variation and concentration levels, Atmos. Chem. Phys.,
653 14, 7807-7823, 2014.
654
655 Hatch, L.E., Creamean, J.M., Ault, A.P., Surratt, J.D., Chan, M.N., Seinfeld, J.H., Edgerton, E.S., Su,
656 Y., and Prather, K.A.: Measurements of isoprene-derived organosulfates in ambient aerosols by
657 aerosol time-of-flight mass spectrometry - Part 1: Single particle atmospheric observations in Atlanta,
658 Environ. Sci. Technol., 45, 5105-5111.
659
660 Hayes, P.L., Ortega, A.M., Cubison, M.J., Froyd, K.D., Zhao, Y., Cliff, S.S., Hu, W.W., Toohey,
661 D.W., Flynn, J.H., Lefer, B.L., Grossberg, N., Alvarez, S., Rappenglück, B., Taylor, J.W., Allan, J.D.,
662 Holloway, J.S., Gilman, J.B., Kuster, W.C., De Gouw, J.A., Massoli, P., Zhang, X., Liu, J., Weber,
663 R.J., Corrigan, A.L., Russell, L.M., Isaacman, G., Worton, D.R., Kreisberg, N.M., Goldstein, A.H.,
664 Thalman, R., Waxman, E.M., Volkamer, R., Lin, Y.H., Surratt, J.D., Kleindienst, T.E., Offenberg,
665 J.H., Dusanter, S., Griffith, S., Stevens, P.S., Brioude, J., Angevine, W.M., and Jimenez, J.L.: Organic
666 aerosol composition and sources in Pasadena, California, during the 2010 CalNex campaign, J.
667 Geophys. Res. Atmos., 118, 9233-9257, 2013.
668
669 Hawkins, L.N., Russell, L.M., Covert, D. S., Quinn, P. K., and Bates, T. S.: Carboxylic acids, sulfates,
670 and organosulfates in processed continental organic aerosol over the south east Pacific Ocean during
671 VOCALS-REx 2008, J. Geophys. Res.-Atmos., 115, D13201, 2010.
672

673 Hu, K.S., Darer, A.I., and Elrod, M.J.: Thermodynamics and kinetics of the hydrolysis of
674 atmospherically relevant organonitrates and organosulfates, Atmos. Chem. Phys., 11, 8307–8320,
675 2011.
676
677 Hunter, J.F., Carrasquillo, A.J., Daumit, K.E., and Kroll, J.H.: Secondary organic aerosol formation
678 from acyclic, monocyclic, and polycyclic alkanes, Environ. Sci. Technol., 48, 10227-10234, 2014.
679
680 Iinuma, Y., Müller, C., Berndt, T., Böge, O., Claeys, M., and Herrmann, H.: Evidence for the
681 existence of organosulfates from β-pinene ozonolysis in ambient secondary organic aerosol, Environ.
682 Sci. Tech., 41, 6678-6683, 2007.
683
684 Iinuma, Y., Böge, O., Kahnt, A., and Herrmann, H.: Laboratory chamber studies on the formation of
685 organosulfates from reactive uptake of monoterpene oxides, Phys. Chem. Chem. Phys., 11, 7985-
686 7997, 2009.
687
688 Jacobs, M.I., Darer, A.I., and Elrod, M.J.: Rate constants and products of the OH reaction with
689 isoprene-derived epoxides, Environ. Sci. Technol, 43, 12868-12876, 2013.
690
691 Jokinen, T., Sipilä, M., Richters, S., Kerminen, V.-M., Paasonen, P., Stratmann, F., Worsnop, D.,
692 Kulmala, M., Ehn, M., Herrmann, H., and Berndt, T.: Rapid Autoxidation Forms Highly Oxidized
693 RO2 Radicals in the Atmosphere, Angwe. Chem. Internat. Ed., 53, 14596–14600, 2014.
694
695 Kamens, R.M., Zhang, H., Chen, E.H., Zhou, Y., Parikh, H.M., Wilson, R.L., Galloway, K.E., and
696 Rosen, E.P.: Secondary organic aerosol formation from toluene in an atmospheric hydrocarbon
697 mixture: water and particle seed effects, Atmos. Environ., 45, 2324-2334, 2011.
698
699 Kitanovski, Z., Grgic, I., Yasmeen, F., Claeys, M., and Cusak, A.: Development of a liquid
700 chromatographic method based on ultraviolet–visible and electrospray ionization mass spectrometric
701 detection for the identification of nitrocatechols and related tracers in biomass burning atmospheric
702 organic aerosol, Rapid Commun. Mass. Spectrom., 26, 793-804, 2012.
703
704 Kristensen, K., and Glasius, M.: Organosulfates and oxidation products from biogenic hydrocarbons in
705 fine aerosols from a forest in North West Europe during spring, Atmos. Environ., 45, 4546-4556,
706 2011.
707
708 Kroll, J.H., and Seinfeld, J.H.: Chemistry of secondary organic aerosol: formation and evolution of
709 low-volatility organics in the atmosphere, Atmos. Environ., 42, 3593-3624, 2008.

Kuang, B.Y., Lin, P., Hub, M., and Yu, J.Z.: Aerosol size distribution characteristics of organosulfates in the Pearl River Delta region, China, Atmos. Environ., 130, 23-35, 2016.

Kundu, S., Quraishi, T.A., Yu, G., Suarez, C., Keutsch, F.N., and Stone, E.A.: Evidence and quantification of aromatic organosulfates in ambient aerosols in Lahore, Pakistan, Atmos. Chem. Phys., 13, 4865-4875, 2013.

Kwok, E.S.C., and Atkinson, R.: Estimation of hydroxyl radical reaction rate constants for gas-phase organic compounds using a structure-reactivity relationship: an update, Atmos. Environ., 29, 1685-1695, 1995.

Lambe, A.T., Onasch, T.B., Croasdale, D.R., Wright, J.P., Martin, A.T., Franklin, J.P., Massoli, P., Kroll, J.H., Canagaratna, M.R., Brune, W.H., Worsnop, D.R., and Davidovits, P.: Transitions from functionalization to fragmentation reactions of laboratory secondary organic aerosol (SOA) Generated from the OH oxidation of alkane precursors, Environ. Sci. Technol., 46, 5430-5437, 2012.

Lee, S., Jang, M., and Kamens, R. K.: SOA formation from the photooxidation of α-pinene in the presence of freshly emitted diesel soot exhaust, Atmos. Environ., 38, 2597–2605, 2004.

Liao, J., Froyd, K.D., Murphy, D.M., Keutsch, F.N., Yu, G., Wennberg, P.O., St. Clair, J.M., Crounse, J.D., Wisthaler, A., Mikoviny, T., Jimenez, J.L., Campuzano-Jost, P., Day, D.A., Hu, W., Ryerson, T.B., Pollack, I.B., Peischl, J., Anderson, B.E., Ziemba, L.D., Blake, D.R., Meinardi, S., and Diskin, G.: Airborne measurements of organosulfates over the continental U.S., J. Geophys. Res. D, 120, 2990-3005, 2015.

Liggio, J., and Li, S.-M.: Organosulfate formation during the uptake of pinonaldehyde on acidic sulfate aerosols, Geophys. Res. Lett., 33, L13808, 2006.

Lim, Y.B., and Ziemann, P.J.: Products and mechanism of secondary organic aerosol formation from reactions of n-alkanes with OH radicals in the presence of NOx, Environ. Sci. Technol., 39, 9229-9236, 2005.

Lim, Y.B., and Ziemann, P.J.: Effects of molecular structure on aerosol yields from OH radical-initiated reactions of linear, branched, and cyclic alkanes in the presence of NOx, Environ. Sci. Technol., 43, 2328-2334, 2009.

747 Lin, Y.-H., Zhang, Z., Docherty, K.S., Zhang, H., Budisulistiorini, S.H., Rubitschun, C.L., Shaw, S.L.,
748 Knipping, E.M., Edgerton, E.S., Kleindienst, T.E., Gold, A., and Surratt, J.D.: Isoprene epoxydiols as
749 precursors to secondary organic aerosol formation: acid-catalyzed reactive uptake studies with
750 authentic compounds, Environ. Sci. Technol., 46, 250-258, 2012.
751
752 Lin, Y.-H., Budisulistiorini, S.H., Chu, K., Siejack, R.A., Zhang, H., Riva, M., Zhang, Z., Gold, A.,
753 Kautzman, K.E., and Surratt, J.D.: Light-absorbing oligomer formation in secondary organic aerosol
754 from reactive uptake of isoprene epoxydiols, Environ. Sci. Technol., 48, 12012-12021, 2014.
755
756 Loza, C.L., Craven, J.S., Yee, L.D., Coggon, M.M., Schwantes, R.H., Shiraiwa, M., Zhang, X.,
757 Schilling, K.A., Ng, N.L., Canagaratna, M.R., Ziemann, P., Flagan, R.C., and Seinfeld, J.H.:
758 Secondary organic aerosol yields of 12-carbon alkanes, Atmos. Chem. Phys., 7, 1423-1439, 2014.
759
760 Ma, Y., Xu, X., Song, W., Geng, F., and Wang, L.: Seasonal and diurnal variations of particulate
761 organosulfates in urban Shanghai, China, Atmos. Environ., 85, 152-160, 2014.
762
763 Mael, L.E., Jacobs, M.I., and Elrod, M.J.: Organosulfate and nitrate formation and reactivity from
764 epoxides derived from 2-methyl-3-buten-2-ol, J. Phys. Chem. A, 119, 4464-4472, 2015.
765
766 Mentel, T.F., Springer, M., Ehn, M., Kleist, E., Pullinen, I., Kurten, T., Rissanen, M., Wahner, A., and
767 Wildt, J.: Formation of highly oxidized multifunctional compounds: autoxidation of peroxy radicals
768 formed in the ozonolysis of alkenes –deduced from structure–product relationships, Atmos. Chem.
769 Phys., 15, 6745-6765, 2015.
770
771 Mutzel, A., Poulain, L., Berndt, T., Iinuma, Y., Rodigast, M., Böge, O., Richters, S., Spindler, G.,
772 Sipila, M., Jokinen, T., Kulmala, M., and Herrmann, H.: Highly oxidized multifunctional organic
773 compounds observed in tropospheric particles: a field and laboratory study, Environ. Sci. Technol., 49,
774 7754-7761, 2015.
775
776 Ng, N.L., Kwan, A.J., Surratt, J.D., Chan, A.W.H., Chhabra, P.S., Sorooshian, A., Pye, H.O.T.,
777 Crounse, J.D., Wennberg, P.O., Flagan, R.C., and Seinfeld, J.H.: Secondary organic aerosol (SOA)
778 formation from reaction of isoprene with nitrate radicals (NO_3), Atmos. Chem. Phys., 8, 4117-4140,
779 2008.
780 Nozière, B., Ekström, S., Alsberg, T., and Holmström, S.: Radical-initiated formation of
781 organosulfates and surfactants in atmospheric aerosols, Geophys. Res. Lett., 37, L05806, 2010.
782

783 Orlando, J.J., and Tyndall, G.S.: Laboratory studies of organic peroxy radical chemistry: an overview
784 with emphasis on recent issues of atmospheric significance, Chem Rev., 41, 6294-6317, 2012.
785
786 Paulot, F., Crounse, J.D., Kjaergaard, H.G., Kroll, J.H., Seinfeld, J.H., and Wennberg, P.O.: Isoprene
787 photooxidation: New insights into the production of acids and organic nitrates, Atmos. Chem. Phys.,
788 9, 1479-1501, 2009.
789
790 Pratt, K.A., Fiddler, M.N., Shepson, P.B., Carlton, A.G, and Surratt, J.D.: Organosulfates in cloud
791 water above the Ozarks isoprene source region, Atmos. Environ., 77, 231-238, 2013.
792
793 Presto, A.A., Miracolo, M.A., Donahue, N.M., and Robinson, A.L.: Secondary organic aerosol
794 formation from high-NOx Photo-oxidation of low volatility precursors: N-alkanes, Environ. Sci.
795 Technol.,44, 2029-2034, 2010
796
797 Pye, H.O.T., and Pouliot, G.A.: Modeling the role of alkanes, polycyclic aromatic hydrocarbons, and
798 their oligomers in secondary organic aerosol formation, Environ. Sci. Technol., 46, 6041-6047, 2012.
799 Raff, J.D., and Finlayson-Pitts, B.J.: Hydroxyl radical quantum yields from isopropyl nitrite photolysis
800 in air, Environ. Sci. Technol., 44, 8150-8155, 2010.
801
802 Riedel, T.P., Lin, Y., Budisulistiorini, S.H., Gaston, C.J., Thornton, J.A., Zhang, Z., Vizuete, W.,
803 Gold, D., and Surratt, J.D.: Heterogeneous reactions of isoprene-derived epoxides: reaction
804 probabilities and molar secondary organic aerosol yield estimates, Environ. Sci. Technol. Lett., 2, 38-
805 42, 2015.
806
807 Rissanen, M.P., Kurten, T., Sipila, M., Thornton, J.A., Kausiala, O., Garmash, O., Kjaergaard, H.G.,
808 Petaja, T., Worsnop, D.R., Ehn, M., and Kulmala, M.: Effects of chemical complexity on the
809 autoxidation mechanisms of endocyclic alkene ozonolysis products: from methylcyclohexenes toward
810 understanding α-pinene, J. Phys. Chem. A, 119, 4633-4650, 2015.
811
812 Riva, M., Tomaz, S., Cui, T., Lin, Y.-H., Perraudin, E., Gold, A., Stone, E.A., Villenave, E., and
813 Surratt, J.D.: Evidence for an unrecognized secondary anthropogenic source of organosulfates and
814 sulfonates: Gas-phase oxidation of polycyclic aromatic hydrocarbons in the presence of sulfate
815 aerosol, Environ. Sci. Technol., 49, 6654–6664, 2015a.
816 Riva, M., Budisulistiorini, S.H., Zhang, Z., Gold, A., and Surratt, J.D.: Chemical characterization of
817 secondary organic aerosol constituents from isoprene ozonolysis in the presence of acidic aerosol,
818 Atmos. Chem., 130, 5-13, 2016.

819
820 Robinson, A.L., Donahue, N.M., Shrivastava, M.K., Weitkamp, E., Sage, A.M., Grieshop, A. P., Lane,
821 T.E., Pierce, J.R., and Pandis, S.N.: Rethinking organic aerosols: semivolatile emissions and
822 photochemical aging, Science, 315, 1259–1262, 2007.
823
824 Romero, F., and Oehme, M.: Organosulfates – a new component of humic-like substances in
825 atmospheric aerosols?, J. Atmos. Chem., 52, 283-294, 2005.
826
827 Rudzinski, K. J., Gmachowski, L., and Kuznietsova, I.: Reactions of isoprene and sulphoxy radical-
828 anions – a possible source of atmospheric organosulphites and organosulphates, Atmos. Chem. Phys.,
829 9, 2129-2140, 2009.
830
831 Schilling Fahnestock, K.A., Yee, L.D., Loza, C.L., Coggon, M.M., Schwantes, R., Zhang, X.,
832 Dalleska, N.F., and Seinfeld, J.H.: Secondary organic aerosol composition from C12 alkanes, J. Phys.
833 Chem. A, 119, 4281-4297, 2015.
834
835 Schindelka, J., Iinuma, Y., Hoffmann, D., and Herrmann, H.: Sulfate radical-initiated formation of
836 isoprene-derived organosulfates in atmospheric aerosols, Faraday Discuss., 165, 237-259, 2013.
837
838 Schöne, L., Schindelka, J., Szeremeta, E., Schaefer, T., Hoffmann, D., Rudzinski, K.J., Szmigielski,
839 R., and Herrmann, H.: Atmospheric aqueous phase radical chemistry of the isoprene oxidation
840 products methacrolein, methyl vinyl ketone, methacrylic acid and acrylic acid – kinetics and product
841 studies, Phys. Chem. Chem. Phys., 16, 6257–6272, 2014
842
843 Shalamzari, S.M., Ryabtsova, O., Kahnt, A., Vermeylen, R., Hérent, M.-F., Quetin-Leclercq, J., Van
844 Der Veken, P., Maenhaut, W., and Claeys, M.: Mass spectrometric characterization of organosulfates
845 related to secondary organic aerosol from isoprene, Rapid Commun. Mass Spectrom., 27, 784-794,
846 2013.
847
848 Shalamzari, M.S., Kahnt, A., Vermeylen, R., Kleindienst, T.E., Lewandowski, M., Cuyckens, F.,
849 Maenhaut,W., and Claeys, M.: Characterization of polar organosulfates in secondary organic aerosol
850 from the green leaf volatile 3-Z-hexenal, Environ. Sci. Technol., 48, 12671–12678, 2014.
851
852 Shalamzari, M.S., Vermeylen, R., Blockhuys, F., Kleindienst, T.E., Lewandowski, M., Szmigielski,
853 R., Rudzinski, K.J., Spolnik, G., Danikiewicz, W., Maenhaut,W., and Claeys, M.: Characterization of
854 polar organosulfates in secondary organic aerosol from the unsaturated aldehydes 2-E-pentenal, 2-E-
855 hexenal, and 3-Z-hexenal, Atmos. Chem. Phys. Discuss., 15, 29555–29590, 2015.

856
857 Stevens, B., and Boucher, O.: The aerosol effect, Nature, 490, 40-41, 2012.
858
859 Stone, E., Schauer, J., Quraishi, T.A., and Mahmood, A.: Chemical characterization and source
860 apportionment of fine and coarse particulate matter in Lahore, Pakistan, Atmos. Environ., 44, 1062-
861 1070, 2010.
862
863 Stone, E.A., Yang, L., Yu, L.E., and Rupakheti, M.: Characterization of organosulfate in atmospheric
864 aerosols at Four Asian locations, Atmos. Environ., 47, 323-329, 2012.
865
866 Surratt, J.D., Murphy, S.M., Kroll, J.H., Ng, N.L., Hildebrandt, L., Sorooshian, A., Szmigielski, R.,
867 Vermeylen, R., Maenhaut, W., Claeys, M., Flagan, R.C., and Seinfeld, J.H.: Chemical composition
868 of secondary organic aerosol formed from the photooxidation of isoprene, J. Phys. Chem. A, 110,
869 9665-9690, 2006.
870
871 Surratt, J.D., Kroll, J.H., Kleindienst, T.E., Edney, E.O., Claeys, M., Sorooshian, A., Ng, N.L.,
872 Offenberg, J.H., Lewandowski, M., Jaoui, M., Flagan, R.C., and Seinfeld, J.H.: Evidence for
873 organosulfates in secondary organic aerosol, Environ. Sci. Technol., 41, 517-527, 2007.
874
875 Surratt, J.D., Gómez-González, Y., Chan, A.W.H., Vermeylen, R., Shahgholi, M., Kleindienst, T.E.,
876 Edney, E.O., Offenberg, J.H., Lewandowski, M., Jaoui, M., Maenhaut, W., Claeys, M., Flagan, R.C.,
877 and Seinfeld, J.H.: Organosulfate formation in biogenic secondary organic aerosol, J. Phys. Chem. A,
878 112, 8345-8378, 2008.
879
880 Surratt, J.D., Chan, A.W.H., Eddingsaas, N.C., Chan, M., Loza, C.L., Kwan, A.J., Hersey, S.P.,
881 Flagan, R.C., Wennberg, P.O., and Seinfeld, J.H.: Reactive intermediates revealed in secondary
882 organic aerosol formation from isoprene, Proc. Natl. Acad. Sci., 107, 6640-6645, 2010.
883
884 Tao, S., Lu, X., Levac, N., Bateman, A.P., Nguyen, T.B., Bones, D.L., Nizkorodov, S.A., Laskin, J.,
885 Laskin, A., and Yang, X.: Molecular characterization of organosulfates in organic aerosols from
886 Shanghai and Los Angeles urban areas by nanospray-desorption electrospray ionization high-
887 resolution mass spectrometry, Environ. Sci. Technol., 48 (18), 10993-11001, 2014.
888
889 Tkacik, D.S., Presto, A.A., Donahue, N.M., and Robinson, A.L.: Secondary organic aerosol formation
890 from intermediate-volatility organic compounds: cyclic, linear, and branched alkanes, Environ. Sci.
891 Technol., 46, 8773-8781, 2012.
892

Tolocka, M.P., and Turpin, B.: Contribution of organosulfur compounds to organic aerosol mass, Environ. Sci. Technol., 46, 7978-7983, 2012.

Wang, L., Arey, J., and Atkinson, R.: Kinetics and products of photolysis and reaction with OH radicals of a series of aromatic carbonyl compounds, Environ. Sci. Technol., 40, 5465-5471, 2006.

Wang, X.K., Rossignol, S., Ma, Y, Yao, L., Wang, M.Y., Chen, J.M., George, C., and Wang, L.: Identification of particulate organosulfates in three megacities at the middle and lower reaches of the Yangtze River, Atmos. Chem. Phys. Discuss., 15, 21414-21448, 2015.

Witkowski, B., and Gierczak, T.: Analysis of α-acyloxyhydroperoxy aldehydes with electrospray ionization–tandem mass spectrometry (ESI-MSn), J. Mass. Spectrom., 48, 79-88, 2013.

Yao, L., Ma, Y., Wang, L., Zheng, J., Khalizov, A., Chen, M., Zhou, Y., Qi, L., and Cui, F.: Role of stabilized Criegee Intermediate in secondary organic aerosol formation from the ozonolysis of α-cedrene, Atmos. Environ., 94, 448-457, 2014.

Yee, L.D., Craven, J.S., Loza, C.L., Schilling, K.A., Ng, N.L., Canagaratna, M.R., Ziemann, P.J., Flagan, R.C., and Seinfeld, J.H.: Secondary organic aerosol formation from low-NO x photooxidation of dodecane: Evolution of multigeneration gas-phase chemistry and aerosol composition, J. Phys. Chem. A, 116, 6211-6230, 2012.

Yee, L.D., Craven, J.S., Loza, C.L., Schilling, K.A., Ng, N.L., Canagaratna, M.R., Ziemann, P.J., Flagan, R.C., and Seinfeld, J.H.: Effect of chemical structure on secondary organic aerosol formation from C12 alkanes, Atmos. Chem. Phys., 13, 11121-11140, 2013.

Zhang, H., Worton, D.R., Lewandowski, M., Ortega, J., Rubitschun, C.L., Park, J.-H., Kristensen, K., Campuzano-Jost, P., Day, D.A., Jimenez, J.L., Jaoui, M., Offenberg, J.H., Kleindienst, T.E., Gilman, J., Kuster, W.C., De Gouw, J., Park, C., Schade, G.W., Frossard, A.A., Russell, L., Kaser, L., Jud, W., Hansel, A., Cappellin, L., Karl, T., Glasius, M., Guenther, A., Goldstein, A.H., Seinfeld, J.H., Gold, A., Kamens, R.M., and Surratt, J.D.: Organosulfates as tracers for secondary organic aerosol (SOA) formation from 2-methyl-3-buten-2-ol (MBO) in the atmosphere, Environ. Sci. Technol., 46, 9437-9446, 2012.

927 Zhang, X., Schwantes, R.H., Coggon, M.M., Loza, C.L., Schilling, K.A., Flagan, R.C., Seinfeld, J.H.:
928 Role of ozone in SOA formation from alkane photooxidation, Atmos. Phys. Chem., 14, 1733-1753,
929 2014
930
931 Zhang, X., McVay, R.C., Huang, D.D., Dalleska, N.F., Aumont, B., Flagan, R.C., and Seinfeld, J.H.:
932 Formation and evolution of molecular products in α-pinene secondary organic aerosol, Proc. Natl.
933 Acad. Sci., 112, 14168-14173, 2015.
934
935 Ziemann, P.J., and Atkinson, R.: Kinetics, products, and mechanisms of secondary organic aerosol
936 formation, Chem. Soc. Rev., 41, 6582-6605, 2012.

937 **Table 1.** Summary of outdoor smog chamber conditions used for the photooxidation of long-chain alkanes using isopropyl nitrite (IPN) as an OH
938 radical precursor.
939

Hydrocarbons (HCs)	Initial [HC] (ppb)	Chamber Side	Seed aerosol	Initial [IPN] (ppb)	[NO] (ppb)	[O_3] (ppb)	T (K)	RH (%)	Final OA mass (μg m^{-3})	Total Peroxides (μg m^{-3})
Dodecane	412	N	Non-Acidified	215	< 1	512	304-311	49-59	58	*N.d.*
	420	S	Acidified	212	< 1	528	305-311	51-63	65	*N.d.*
Dodecane	422	N	Non-Acidified	215	< 1	507	302-308	15-20	49	*N.d.*
	427	S	Acidified	212	< 1	538	303-308	14-17	53	*N.d.*
Dodecane	397	N	Acidified	215	< 1	506	304-309	45-52	52	15.4
	409	S	Acidified	212	< 1	585	305-310	15-19	59	15.2
Decalin	175	N	Non-Acidified	138	< 1	327	302-309	48-45	204	*N.d.*
	180	S	Acidified	136	< 1	335	302-308	51-49	224	*N.d.*
Decalin	199	N	Non-Acidified	138	< 1	317	305-306	13-13	200	59.7
	204	S	Acidified	136	< 1	328	306-306	13-14	211	75.5
Decalin	N.I.	N	Acidified	138	< 1	319	302-306	43-54	245	43.9
	N.I.	S	Acidified	136	< 1	324	301-306	9-12	270	57.8
Cyclodecane	257	N	Non-Acidified	172	< 1	374	298-301	53-61	218	76.6
	263	S	Acidified	170	< 1	364	299-301	52-60	238	72.2
Cyclodecane	256	N	Non-Acidified	172	< 1	350	300-303	13-15	177	57.8
	261	S	Acidified	170	< 1	332	300-302	13-14	210	68.3
Cyclodecane	245	N	Acidified	172	< 1	345	298-300	10-11	259	78.8
	250	S	Acidified	170	< 1	355	299-300	51-49	270	69.2

940 *N and S design "North chamber" and "South Chamber", respectively; N.I.: No Information, N.d. Not determined*
941

Table 2. Concentrations (ng m^{-3}) of OSs identified in laboratory-generated dodecane, decalin and cyclodecane SOA and in fine aerosol collected from two urban locations.

		Lahore, Pakistan					Pasadena, USA							
$[M - H]^-$	Precursors	04-30-2007	05-06-2007	05-12-2007	11-02-2007	11-08-2007	05-17-2010	05-18-2010	05-19-2010	05-23-2010	05-24-2010	05-25-2010	05-28-2010	06-11-2010
$C_7H_{13}O_5S^-$ (209.0472)[a,b]	Dodecane	7.53	6.53	4.24	6.35	9.66	*N.d.*	*N.d.*	0.27	0.07	0.10	*N.d.*	0.09	0.21
$C_9H_{17}O_5S^-$ (237.0786)[a,b]	Dodecane	9.35	6.81	4.27	7.27	12.40	0.13	0.15	0.30	0.10	0.16	0.16	0.13	0.25
$C_{10}H_{19}O_5S^-$ (251.0946)[a,c]	Cyclodecane	10.40	7.51	4.08	13.17	20.96	*N.d.*	*N.d.*	*N.d.*	*N.d.*	*N.d.*	*N.d.*	*N.d.*	*N.d.*
$C_{10}H_{17}O_6S^-$ (265.079)[a,c]	Cyclodecane	2.83	2.45	2.15	2.86	7.63	0.18	0.21	0.35	0.14	0.15	0.16	0.15	0.36
$C_9H_{15}O_7S^-$ (267.0554)[a,c]	Decalin	0.98	1.87	1.93	2.19	6.53	0.21	0.21	0.58	0.11	0.21	0.20	0.16	0.40
$C_9H_{17}O_7S^-$ (269.0700)[a,b]	Decalin	2.04	3.02	2.22	2.62	7.56	0.42	0.38	0.58	0.26	0.40	0.38	0.35	0.56
$C_{10}H_{15}O_7S^-$ (279.0556)[a,c]	Cyclodecane	6.38	20.25	21.97	15.06	35.93	0.14	0.21	0.54	0.10	0.19	0.21	0.20	0.29
$C_{12}H_{23}O_5S^-$ (279.1272)[c,d]	Dodecane	14.57	12.18	3.41	9.50	19.56	*N.d.*	*N.d.*	*N.d.*	*N.d.*	*N.d.*	*N.d.*	*N.d.*	*N.d.*
$C_9H_{17}O_8S^-$ (285.0651)[a,c]	Decalin	*N.d.*	0.61	*N.d.*	*N.d.*	1.44	0.20	0.09	0.21	0.05	0.08	0.09	0.03	0.17
$C_{10}H_{15}O_8S$- (295.0500)[a,c]	Decalin	*N.d.*	0.53	0.48	0.54	3.78	0.17	0.22	0.65	0.08	0.17	0.24	0.19	0.52
$C_{10}H_{17}O_8S^-$ (297.0650)[a,c]	Decalin	*N.d.*	0.78	0.92	0.69	*N.d.*	0.13	0.08	0.43	0.07	0.10	0.09	0.10	0.24
$C_{10}H_{16}NO_9S^-$ (326.0550)[a,c]	Decalin	0.25	0.32	0.21	*N.d.*	*N.d.*	*N.d.*	0.13	0.22	0.06	0.09	0.11	0.12	0.11

[a] Quantified using authentic OS (3-pinanol-2-hydrogen sulfate, $C_9H_{13}O_6S^-$), [b] OSs belonging to group 2, [c] OSs belonging to group 1, [d] quantified using octyl sulfate OS ($C_8H_{17}O_4S^-$). Different isomers for one ion have been summed; N.d.: not detected.

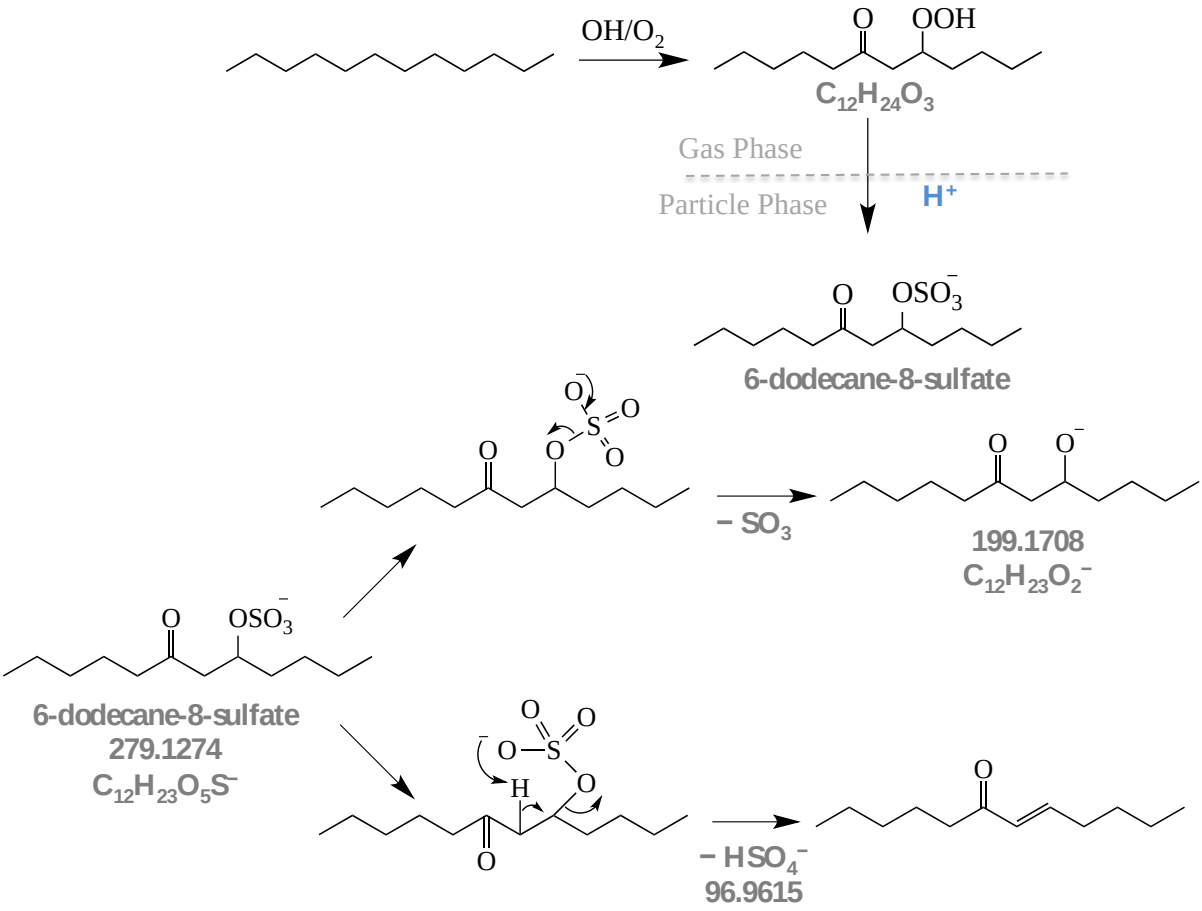

Figure 1. Proposed formation pathway of OS-279 (*m/z* 279.1274) and its corresponding fragmentation routes. The suggested mechanism is based on identified products from previous study (Yee et al., 2012).

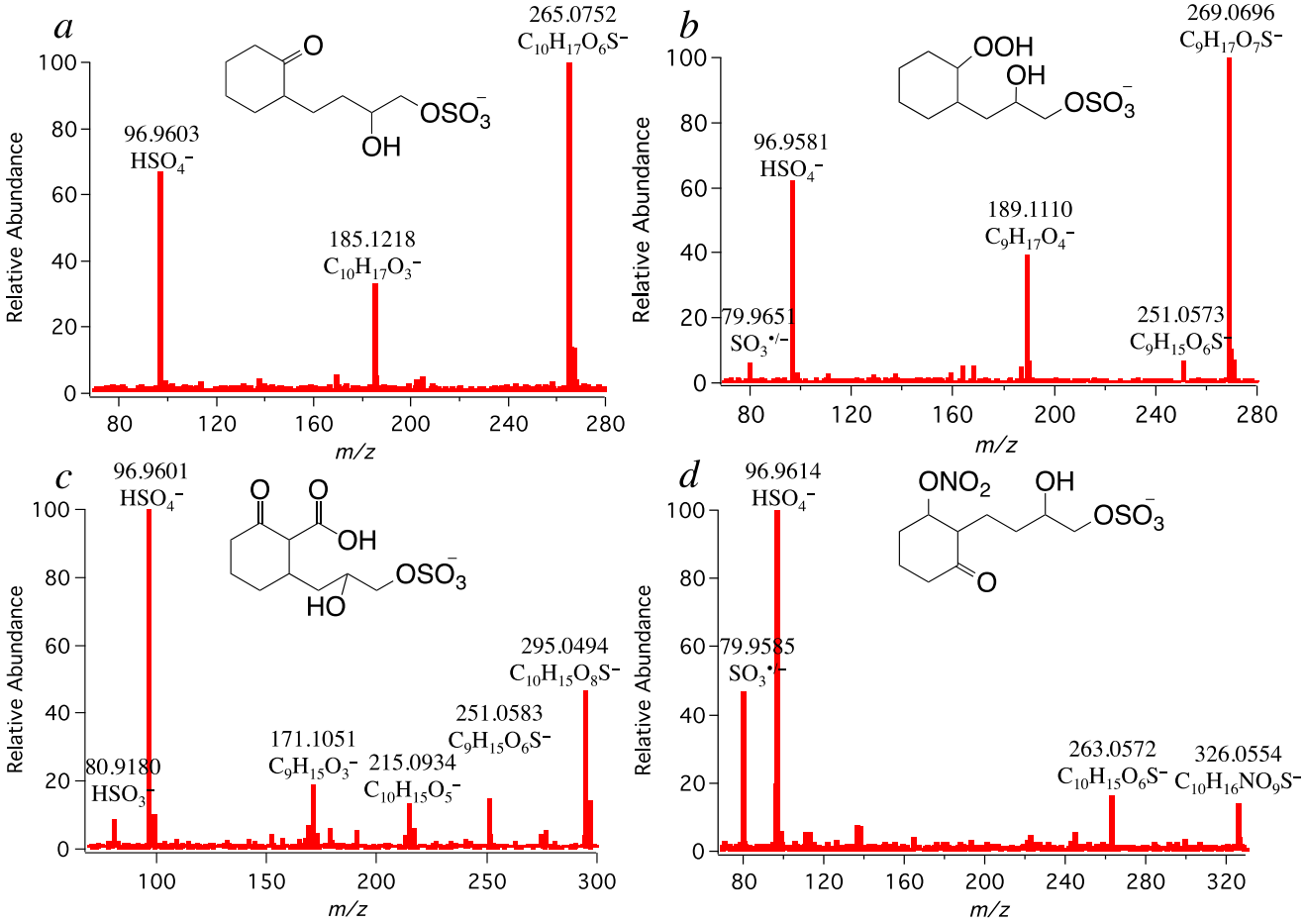

Figure 2. MS^2 spectra obtained for selected decalin-derived OSs: (*a*) *m/z* 265.0752 ($C_{10}H_{17}O_6S^-$), (*b*) *m/z* 269.0696 ($C_9H_{17}O_7S^-$), (*c*) *m/z* 295.0494 ($C_{10}H_{15}O_8S^-$) and (*d*) *m/z* 326.0554 ($C_{10}H_{16}NO_9S^-$). Fragmentation schemes are proposed in Figure S2.

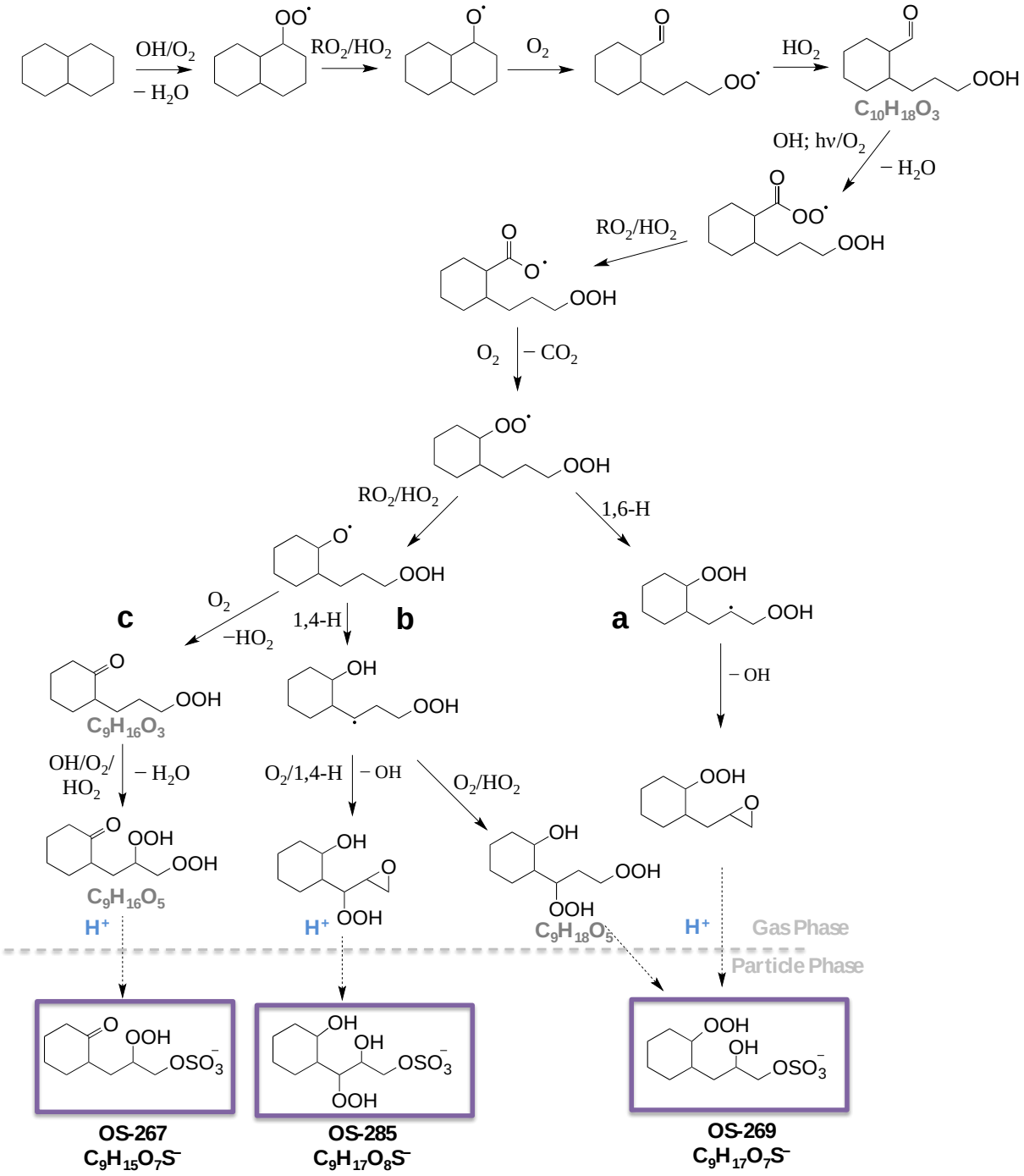

Figure 3. Tentatively proposed formation pathways of OS-267 (*m/z* 267.9552), OS-269 (*m/z* 269.0696) and OS-285 (285.0654) from the oxidation of decalin in presence of sulfate aerosol.

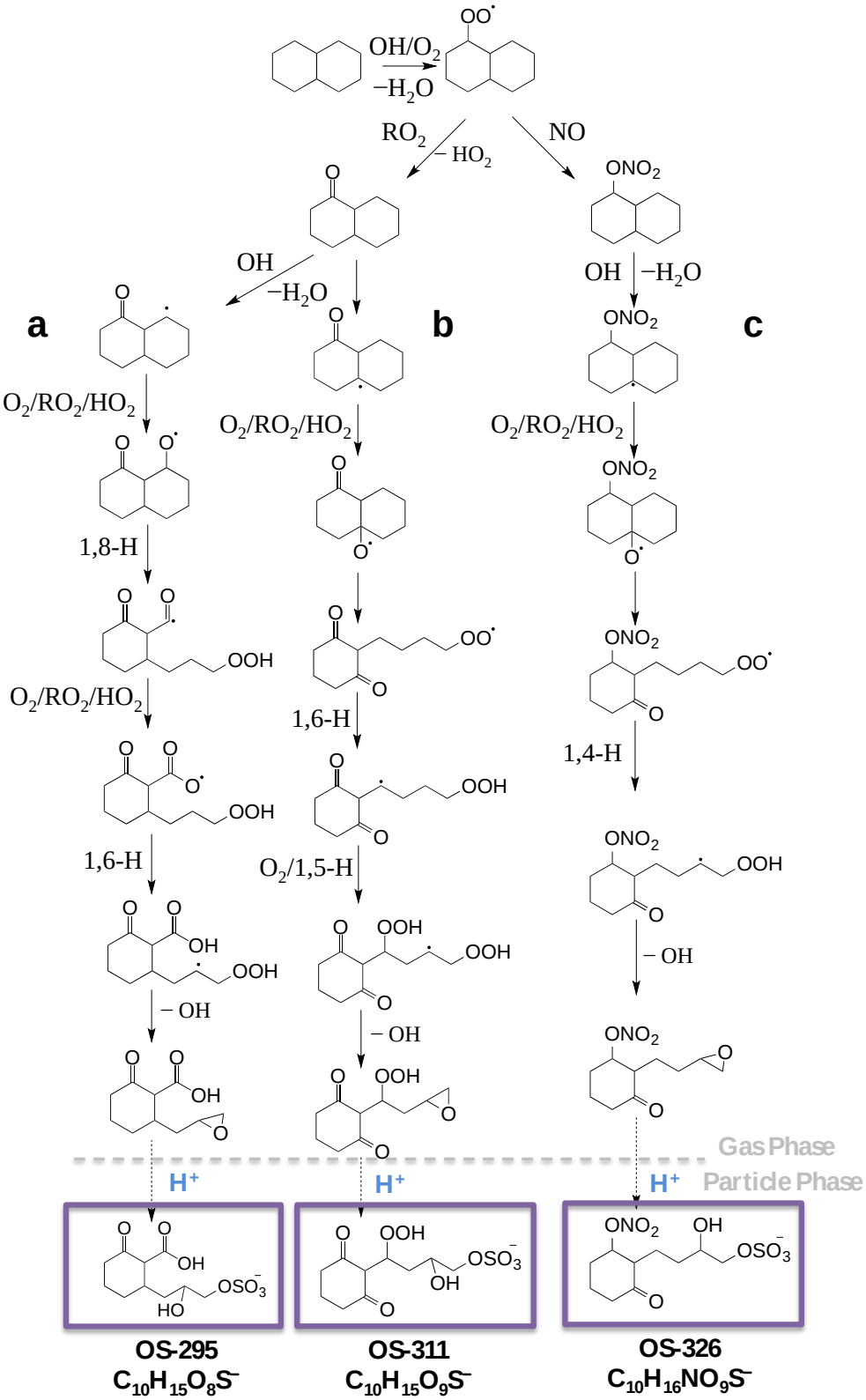

Figure 4. Tentatively proposed formation pathways of OS-295 (295.0494), OS-311 (*m/z* 311.0447) and OS-326 (326.0554) from the oxidation of decalin in the presence of sulfate aerosol.

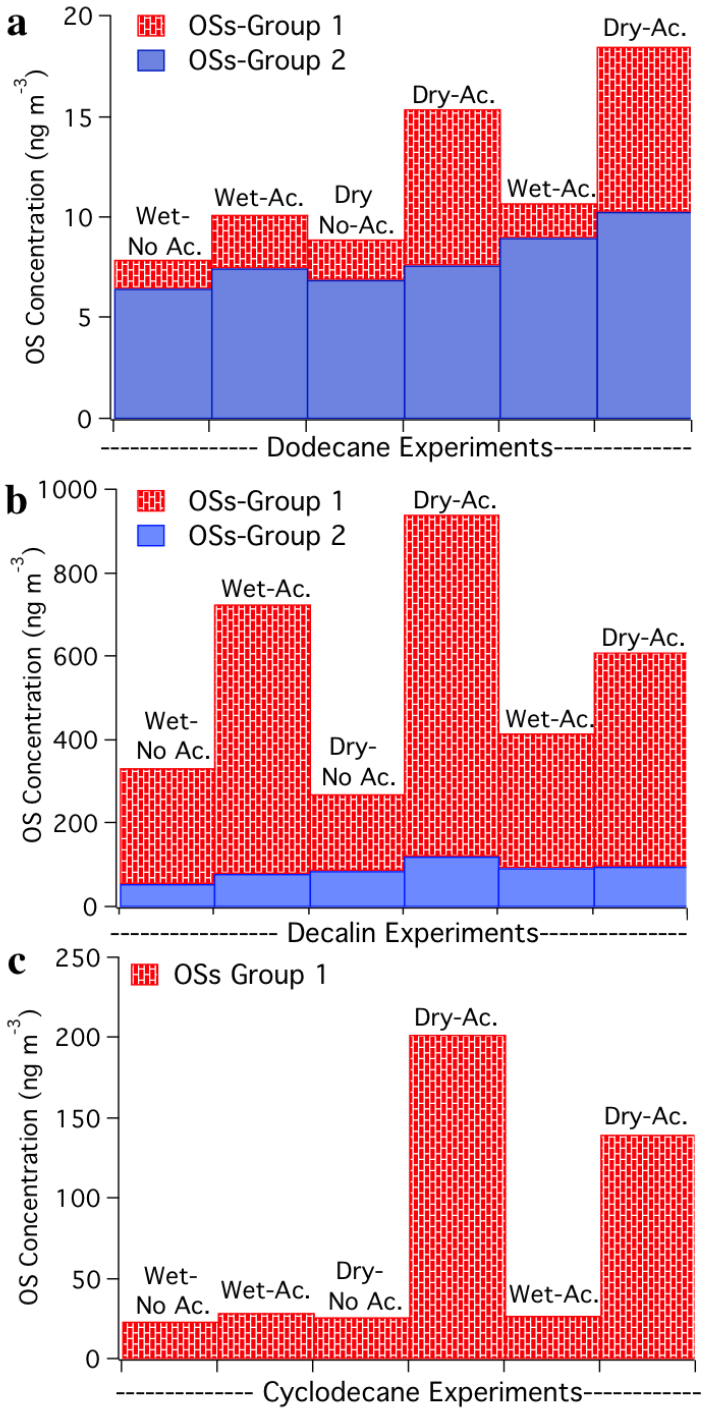

Figure 5. Impact of acidity on OS formation from gas-phase oxidation of (a) dodecane, (b) decalin, and (c) cyclodecane. OSs from Group-1 corresponds to compounds strongly impacted by aerosol acidity, while OSs from Group-2 appeared to have less dependency on aerosol acidity.

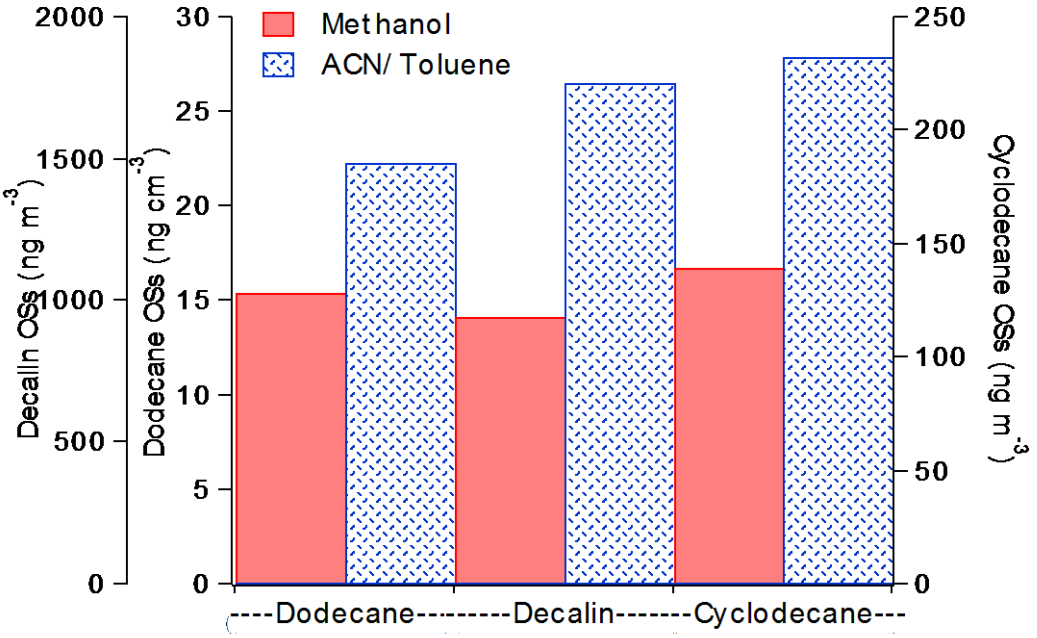

Figure 6. Impact of extraction solvent composition on quantification of identified OSs from gas-phase oxidation of alkanes.

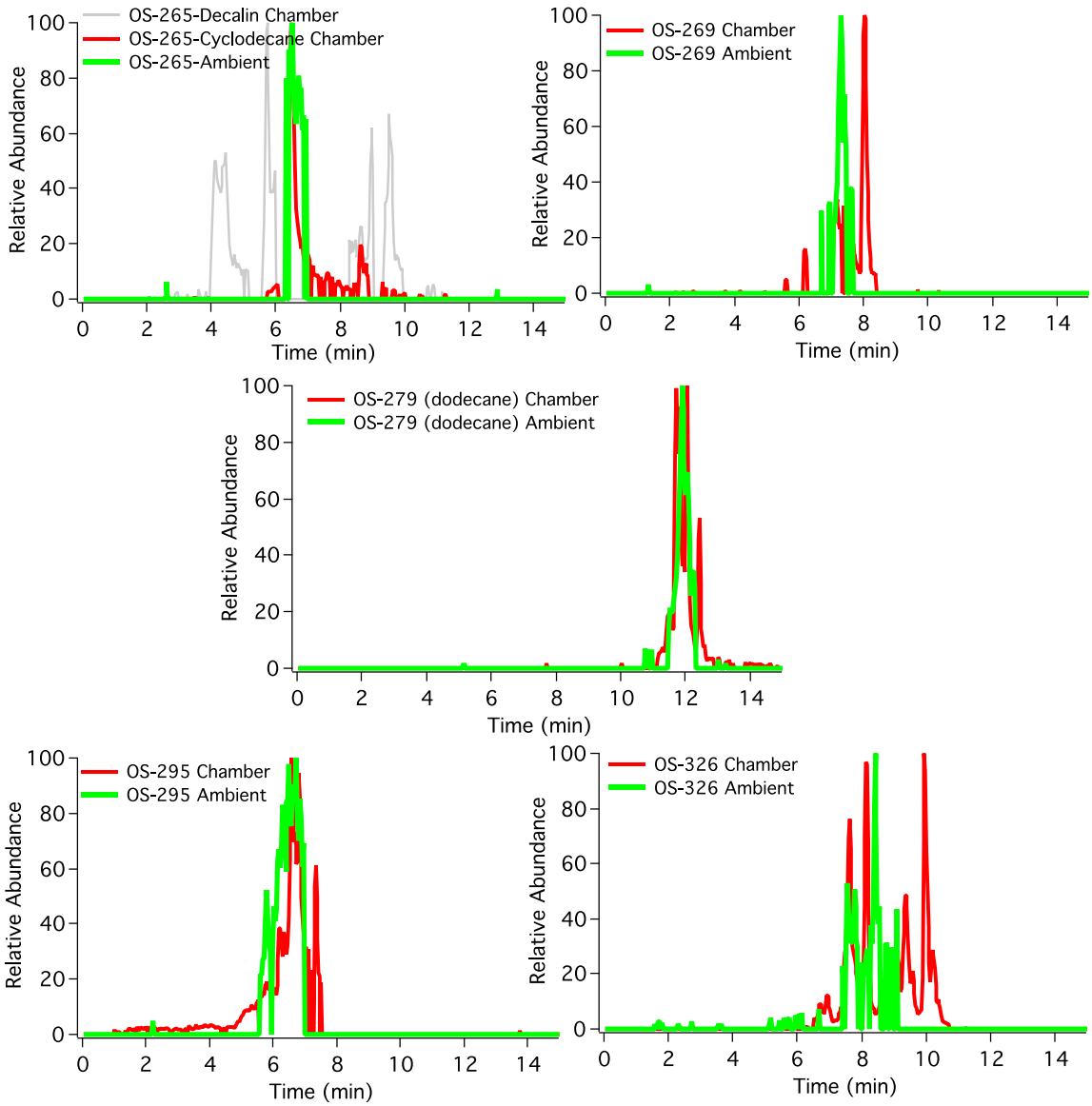

Figure 7. Extracted ion chromatograms (EICs) for selected alkane OSs identified in both smog chamber experiments (in red) and ambient samples (in green).